8-18-2016

QM/MM Calculations of Spectral Tuning in Squid Rhodopsin

Jennifer Pardus
jpardus@comcast.net

QM/MM Calculations of Spectral Tuning in Squid Rhodopsin

Jennifer Lynn Pardus

B.S., The University of Connecticut, 1998

A Thesis

Submitted in Partial Fulfillment of the

Requirements for the Degree of

Master of Science

At the

University of Connecticut

2016

APPROVAL PAGE

Master of Science Thesis

QM/MM Calculations of Spectral Tuning in Squid Rhodopsin

Presented by

Jennifer Lynn Pardus, B.S.

Major Advisor Dr. José A. Gascón

Associate Advisor Dr. Alfredo Angeles-Boza

Associate Advisor Dr. Amy Howell

University of Connecticut

2016

Abstract

This study utilized a QM/MM methodology to model and explore the protein structure and active site of invertebrate squid rhodopsin, and employed time dependent density functional theory (td-dft) calculations to further investigate the excited states of this protein. The high-resolution (2.5 Å) X-ray crystal structure of squid rhodopsin (species Todarodes pacificus) was the first Gq-coupled Guanine Protein Coupled Receptor (GPCR) structure to be determined. The availability of this novel x-ray structure data, in conjunction with computational tools, provided the opportunity to study the relationship between certain structural attributes of squid rhodopsin in the vicinity of the photoreactive center, and the absorption properties of this light sensitive molecule.

This study found that computational results varied depending upon the choice of computational parameters used. Results varied significantly when the definition of the quantum region was modified between experiments. Therefore, absolute comparison of the change in energy (ΔE) between optimized Todarodes pacificus rhodopsin models was found to be inappropriate and conclusions were difficult to draw.

Because of these issues this study was expanded to include other species of squid, and a more meaningful study subsequently emerged through the *relative* comparison of computational results between species. The study was broadened to include the squid species Loligo forbesii and Alloteuthis subulata, in addition to Todarodes pacificus. By

replacing key active center residues in the Todarodes pacificus model with key residues from these other species, and by keeping computational parameters constant between experiments, experimental absorption shifts between species were replicated.

Acknowledgements

I would like to express my sincere gratitude to my advisor, Dr. José Gascón, for all of the valuable instruction and guidance he has generously provided to me in this area of chemistry, and also for his boundless patience, without which I would never have been able to reach my goal. He is a wonderful teacher and person, and I cannot thank him enough for always leaving the door of opportunity open throughout my extended endeavors to complete this project.

I would like to thank my associate advisors Dr. Alfredo Angeles-Boza and Dr. Amy Howell for their valuable time spent in reviewing my thesis and participating in the defense presentation process. I would like to thank Laura Stone of the Graduate School for her understanding and kindness, and for her help in navigating through the requirements to complete the degree. I am also grateful for the assistance that I received from Sandra Cyr of the Gradate School in preparing the required forms for graduation. And lastly, I want to thank current and former members of the Gascón lab for all of their encouragement and support, with very special thanks going out to Lochana Menikarachchi, Neranjan Perera, Dan Sandberg, and Melinda Samaraweera for sharing their insights on my topic, and for all of the technical assistance they provided to me with the computational programs needed to carry out calculations. I could not have completed this work without their help.

TABLE OF CONTENTS

Chapter 1 – Introduction

1.1 Molecular Modeling and Quantum Mechanics

The research discussed in this report focuses on the use of molecular modeling to gain insight into the structure and chemical properties of squid rhodopsin. While we know that rhodopsin plays an intermediary role between the absorption of light and the generation of electrical signals responsible for vision, the availability of a detailed molecular structure and computational chemistry programs allows one to better understand how and why this process occurs.

The molecular modeling software employed in this study is Gaussian Program software [4], an ab initio quantum chemistry program that is used to predict molecular structures and energies. 'Ab initio' is the Latin term for the adverb 'from the beginning' and is used in chemistry as an adjective to describe calculations that are based on 'first principles' and rely on the basic laws of nature. Quantum mechanics is a level of theory that treats molecules as collections of nuclei and electrons, using complex equations that describe the quantum state and behavior of particles. This theory differs from the molecular mechanics level of theory that treats molecules as a collection of atoms and bonds, using simpler algebraic equations and classical mechanics laws that do not work well in describing very small masses and small transfers of energy [5] [6]. As such, quantum mechanics is the more appropriate level of theory to use for analyzing atomic and

subatomic particles [6], especially those that are directly involved in reactions of a molecule [7].

1.2 The Schrodinger Equation and Approximations

The foundation of ab initio quantum mechanical calculations is the Schrodinger equation, a partial differential equation that describes the quantum state or wavefunction ψ of a chemical system as:

$$H\psi = E\psi$$

where H is the Hamiltonian operator that carries out an operation on the function ψ and returns the energy of the system, E [6] [8].

For a particle of mass m moving in one dimension with energy E, the Schrodinger equation is written as:

$$H\psi = \left(\frac{-\hbar^2}{2m}\right)\left(\frac{d^2\psi}{dx^2}\right) + V(x)\psi = E\psi$$

[6, 8] where ψ is the wavefunction, V is the potential energy of the particle dependent on position x, the first term $(-\hbar^2/2m)(d^2\Psi/dx^2)$ is the kinetic energy of the particle, and $\hbar$ is a modification of Planck's constant h:

$$\hbar = \frac{h}{2\pi} = 1.05457 \times 10^{-34}\ \text{J s}$$

The Schrodinger equation does not specify the position nor the path of an electron, but rather gives the probability of finding an electron within a given region of space [9]. However, only very simple systems can be analytically solved by the Schrodinger

equation [8]. While the Schrodinger equation can be solved exactly for the hydrogen atom [9], many electron atoms in which all of the electrons interact with each other are much too complicated to be solved by this equation, and approximations have to be made [6]. Using Gaussian Program software [4], we employed the following approximation methods in our study: the Hartree-Fock approach (HF) and density functional theory (DFT) for ground state geometry optimizatons; time-dependent density functional theory (TD-DFT) for excited state calculations.

Averting calculation of multiple electron-electron interactions, the Hartree-Fock method treats each electron *independently* moving in an average field of all other electrons and the nuclei [3]. While this approach makes HF a more practical method for calculating the quantum state of a system, the fact that explicit electron-electron interactions are neglected undermines the method's ability to determine accurate wavefunctions and properties [3] [8]. When the HF method was used in the current research, it was employed to obtain a preliminary geometry optimization, and was followed by use of DFT to obtain more accurate results.

Interactions between identical particles (exchange interactions) and interactions between electrons (correlation interactions), neglected by the HF approach, are included in DFT, an approach which relies on the electron density of a system [3]. While the Schrodinger equation and the Hartree-Fock methods optimize wavefunctions,

DFT optimizes electron density [8]. Ground-state density functional theory relies on the Hohenberg-Kohn (HK) theorems and on the existence of a noninteracting reference system. The first Hohenberg-Kohn theorem (HK1) defines the ground-state wave function $\psi(r)$ as a functional of electron density ψ[n](r) [3]. Electron density determines an external potential, which in turn determines the Hamiltonian and wavefunction, from which energy can be computed. This approach however still requires solving of the complicated Schrodinger equation [8]. The second Hohenberg-Kohn theorem (HK2), in combination with HK1, is used to derive the Kohn-Sham (KS) equations and a theory that relies on density, rather than the wavefunction, as the fundamental quantity [3].

Simplified, the total ground state energy (E) for N electrons, using DFT, is as follows [10]:

$$E = T_s + U + E_{xc} + V_{ext}$$

- T_s is the kinetic energy of Kohn-Sham electrons:

$$T_s = \sum_{\sigma} \sum_{j=1}^{N_\sigma} \int d^3r \frac{1}{2} \left| \nabla \phi_{j\sigma}(r) \right|^2$$ N_σ = the number of spin σ electrons

- U is the Hartree energy:

$$U[n] = \frac{1}{2} \sum_{\sigma\sigma'} \int d^3r d^3r' \frac{n_\sigma(r) n_{\sigma'}(r')}{|r - r'|}$$ n(r) = the ground state density of Fermions

- E_{xc} is the exchange-correlation energy:

$$E_{xc}[n_\sigma, n_\beta] = T[n_\sigma, n_\beta] - T_s[n_\sigma, n_\beta] + V_{ee}[n_\sigma, n_\beta] - U[n]$$

$n_\sigma(r)$ and $n_\beta(r)$ are spin densities, with $\sigma,\beta = \pm 1/2$

- V_{ext} is the external potential energy

Time-dependent density functional theory (TDDFT), based on the Runge-Gross theorems, employs the same principles found in DFT, but with the aim of solving time-dependent problems such as those involved with electronic excitations. As with DFT, the complicated Schrodinger equation is replaced with a simpler set of equations, this time with the time-dependent Kohn-Sham equations (TDKS), single particle equations that return time-dependent density [10].

1.3 Rhodopsin and Squid Rhodopsin

Rhodopsin belongs to the largest class (class A, or 'Rhodopsin-like') within the Guanine Protein Coupled Receptor (GPCR) family [11]. A GPCR is a cell membrane protein that acts as an intermediary between an extracellular signal (in rhodopsin's case, light) and an inner cellular guanine nucleotide-binding protein or 'G-protein', making a connection between the two by responding to the outer signal -- usually through a conformational change of the GPCR -- and in turn, binding and activating the G-protein [12] [13]. The conformational change in rhodopsin begins with isomerization of the 11-cis configuration of rhodopsin's chromophore retinal, upon exposure to light, to an all-trans configuration [14] (Figure 1.1).

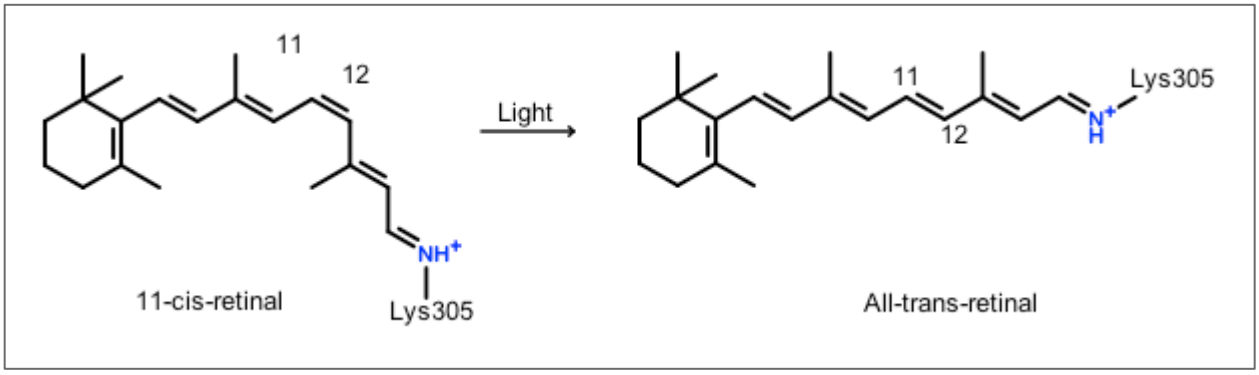

Figure 1.1 – Isomerization in chromophore retinal upon absorption of photon.

Subsequent activation of a G-protein affects a further chain of signaling events, and in rhodopsin these signaling events lead to the generation of electrical signals responsible for vision [12] [13]. In vertebrates, the isomerization from a cis configuration to an all-trans configuration is followed by a series of reactions whereby retinal is dissociated from the opsin protein. However in squid rhodopsin this dissociation does not occur. Instead the stereoisomerization is reversible [92]

Squid rhodopsin (Figure 1.2) belongs to the invertebrate $G_{\alpha q}$-opsin subfamily of rhodopsin [15], opsins that act upon $G_{\alpha q}$-type G-proteins [16] [17] [18]. The target of an activated $G_{\alpha q}$ protein is the enzyme phospholipase C which, once activated itself, catalyses the hydrolysis of PIP_2 (phosphatidyl-inositol-bisphosphate) into IP_3 (inositol-1,4,5-tris phosphate) and DAG (diacylglycerol) [15] [17] [19] [20] [21] [22] [23] [24]. The production of IP_3 leads to a release of calcium ions and a resulting increase in

membrane conductance and depolarization of the photoreceptor membrane from which electrical signals are generated [12] [15] [19] [25] [26].

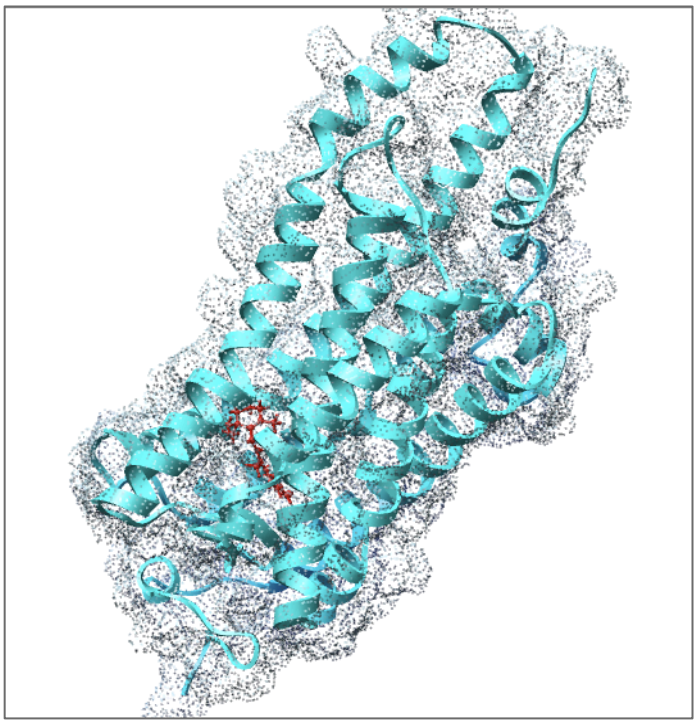

Figure 1.2 - Squid rhodopsin structure from pdb file 2z73

The squid rhodopsin molecule consists of the protein opsin attached to the chromophore retinal (Figure 1.3) [14] [27], with the protein's alpha-helical segments I through VII crossing the cell membrane seven times [28] [29] [30, 31], and two additional helixes, VIII and IX, extending into the cytoplasmic region [2]. While retinal can form many isomers, in the dark most opsins preferentially bind 11-cis-retinal [15]. The molecular weight of rhodopsin in the squid species Todarodes pacificus is 49833 amu, with 448 amino acid residues in the protein structure [32]. The molecular weight of

the chromophore retinal is 282 amu, and its structure is $C_{19}H_{27}CHO$ [33]. Retinal is a metabolite of Vitamin A (Retinol, $C_{19}H_{27}CH_2OH$).

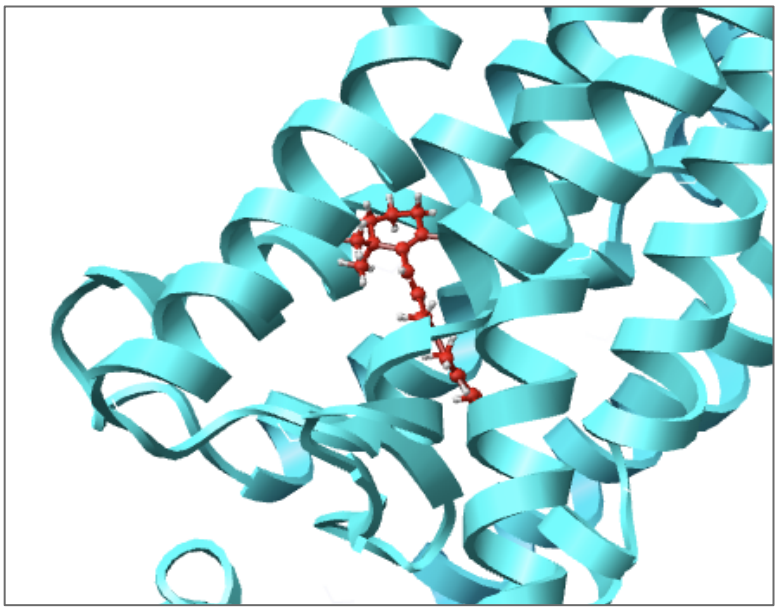

Figure 1.3 - Chromophore retinal (red) nestled in protein opsin helices

Retinal is bound to opsin at one of the protein's lysine residues [30] via a protonated Schiff base linkage [34] [35] [36] [37]. The connection in bovine rhodopsin is at Lys 296 [38] [39], and in squid rhodopsin it is at Lys 305 in helix VII [32] [40]. The positive charge of the protonated Schiff base linkage is stabilized by a nearby negatively charged counterion [15], reported to be Glutamic acid 113 in bovine rhodopsin [41] and Glutamic acid 180 in squid rhodopsin [42] [43].

Rhodopsin is a visual pigment that is responsible for low light vision in vertebrates and is found in the rod photoreceptor cells of vertebrate retina; it is responsible for both dim and bright light vision in invertebrates and is found in the rhabdomeric photoreceptor

cells of invertebrate retina [15] [19] [26] [44] [45] [33, 46] [47, 48]. In squid and other invertebrate eyes, rhodopsin is located in highly ordered microvillar photoreceptor membranes in the retina [19, 46, 47], and these microvilli are tightly packed into light absorbing rhabdomeres, structures that have a large light-absorbing area that helps to support vision in the dim light of deeper ocean waters. Rhabdomeric photoreceptors also adapt very well to bright light, thereby supporting vision in surface waters as well [26].

1.4 Water Molecules and Rhodopsin's Photoreactive Center

Water molecules, while abundantly present in protein crystals, are often not visible in an electron density map produced by x-ray diffraction and thus often not present in a protein's pdb file coordinates. Solvent molecules occupy approximately 27-65% of the volume of a protein crystal [46], and water will attempt to occupy all space in a protein not occupied by protein atoms [47], but the visibility of a water molecule in an electron density map produced through x-ray diffraction strongly depends on the water molecule's motion. If molecular motion is restricted by protein environment, detection of the water molecule by x-ray diffraction is more favorable. For example if the water molecule is in a molecular crevice, especially one that is narrow, the molecule may experience a longer residence time and restricted motion. If the water is interacting with a hydrophilic group, or interacting with polar groups through hydrogen bonding, the water molecule's motion may be limited [47]. Well-ordered water molecules are those

with restricted motions, stronger binding and preferential binding sites and are those that are visible in an electron density map [48].

One of the objectives of this study was to explore the possibility of the presence of a water molecule near the active site of Todarodes pacificus rhodopsin, a water molecule not present in the protein's associated pdb file. To probe this question, we added a water molecule, in the proximity of retinal, to some of our models (Figure 1.4).

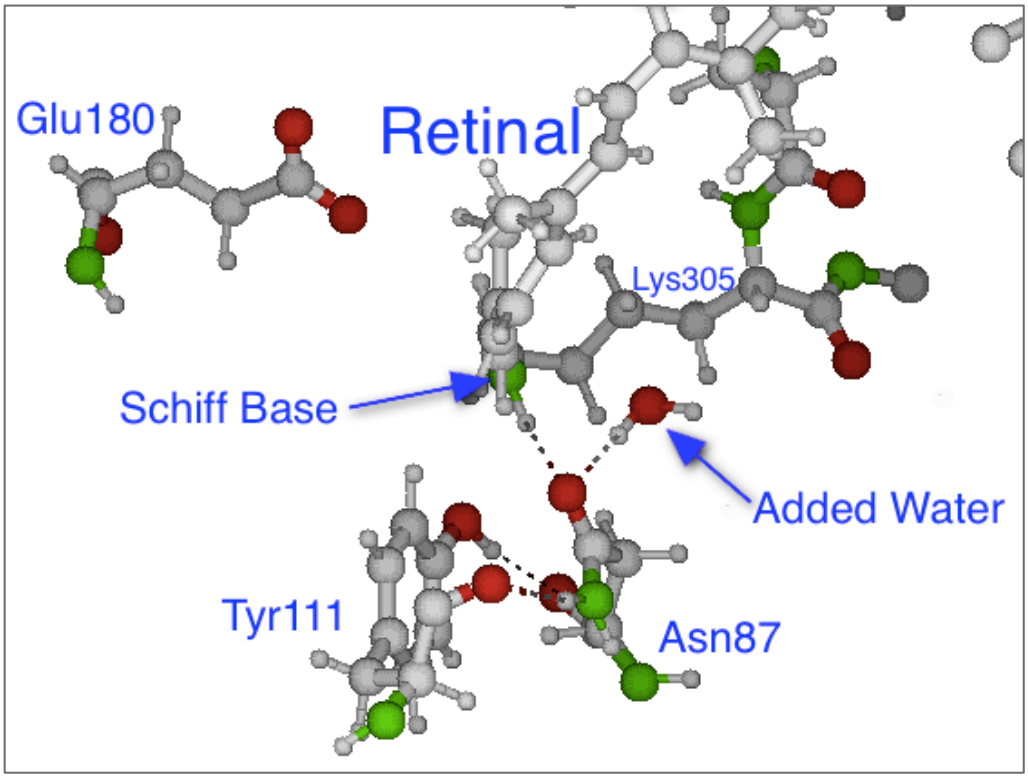

Figure 1.4 – Water molecule added to the model of Todarodes pacificus in the vicinity of retinal, the protonated Schiff base, and Asn87.

The presence of a water molecule is of interest because water molecules play an important role in the activation of rhodopsin, as the following research illustrates. Wald et al showed that dry bovine rhopdosin, while activated upon the absorption of light, becomes stable in the meta rhodopsin intermediate state and does not proceed to regenerate retinal and protein. However, upon addition of water to the dry bovine rhodopsin sample, rhodopsin continues the photocyle process [49]. Using molecular dynamics simulations combined with NMR studies on bovine rhodopsin, Grossfield et al showed that there is a dramatic increase in rhodopsin internal hydration commencing with the initial isomerization of retinal and continuing to the formation of the Meta I intermediate state [50]. Angel et al compared the transmembrane region of five different rhodopsin-like GPCR structures. Ordered waters were found to colocalize amongst the five investigated structures, and were also found to interact with highly conserved residues, suggesting that water plays a significanct role in protein activation [51]. One of the waters in Angel's study was within 3.8 Å of Glu180 and Asn185 [51]. The waters from several of the clusters studied by Angel are part of extended hydrogen-bonded water networks, or 'water wires', and may represent a pathway connecting the proton donor site on the cytoplasmic face of the receptor with an acceptor site in the helicle bundle. These water wires permit more rapid and controlled transmission of protons than diffusion [51]. Molecular dynamics simulations of squid rhodopsin performed by Jardon-Valadez et al show that water molecules have compatible interactions with the side chains of residues in the interhelical region, and participate in a hydrogen bond

network that extends from Asp80 in the interhelical region to Tyr315 at the cytoplasmic face of the protein [52]. Okada's research on the X-ray crystal structure of *bovine* rhodopsin revealed the presence of eight water molecules in the transmembrane region of bovine rhodopsin, two in the vicintiy of the retinal Schiff base and its associated counterion. In conjunction with a hydrogen-bond network, the two water molecules near retinal are proposed to be involved in stabilization of the protonated Schiff base, and involved with the spectral tuning and activation of the chromophore [53] [54]. X-ray crystallography studies of *squid* rhodopsin have shown that there are many more water molecules in squid rhodopsin than there are in bovine rhodopsin, with nine waters in the interhelical cavity region alone. In conjunction with the inner cavity hydrophillic residues Asp80 and Asn311, these water molecules are part of a hydrogen-bonding network that extends from the retinal area to Tyr315 at the cytoplasmic face of the protein [2]. Low temperature FTIR spectroscopy performed by Ota et al suggest that there is also a water molecule in squid rhodopsin that is located between the chromophore's Schiff base and the purported counterion Glu180 [55].

1.5 Counterions in Rhodopsin

Another area of interest in the current study was to investigate the residue Glutamic acid-180 (Glu180) and its asserted role as counterion in squid rhodopsin and in stabilizing the positive charge of the protonated Schiff base linkage [42] [43]. The counterion in *bovine* rhodopsin has previously been demonstrated to be Glu113 [41], a

residue located in the same area where a Tyrosine residue (Tyr111), rather than a Glutamic acid residue, is located in squid rhodopsin. Some doubt has been expressed that Glu180 could be an effective counterion, on it's own, in invertebrate rhodopsin due to its distance from the Schiff base nitrogen (Figure 1.5), and it has been instead suggested that the nearby Asn185 perhaps facilitates an interaction between the Schiff Base nitrogen and Glu180 [2]. Given the location of the counterion in bovine rhodopsin, the question also arises as to whether Tyr111 (i.e. a tyrosinate) could have the anionic properties to serve the counterion purpose in squid rhodopsin.

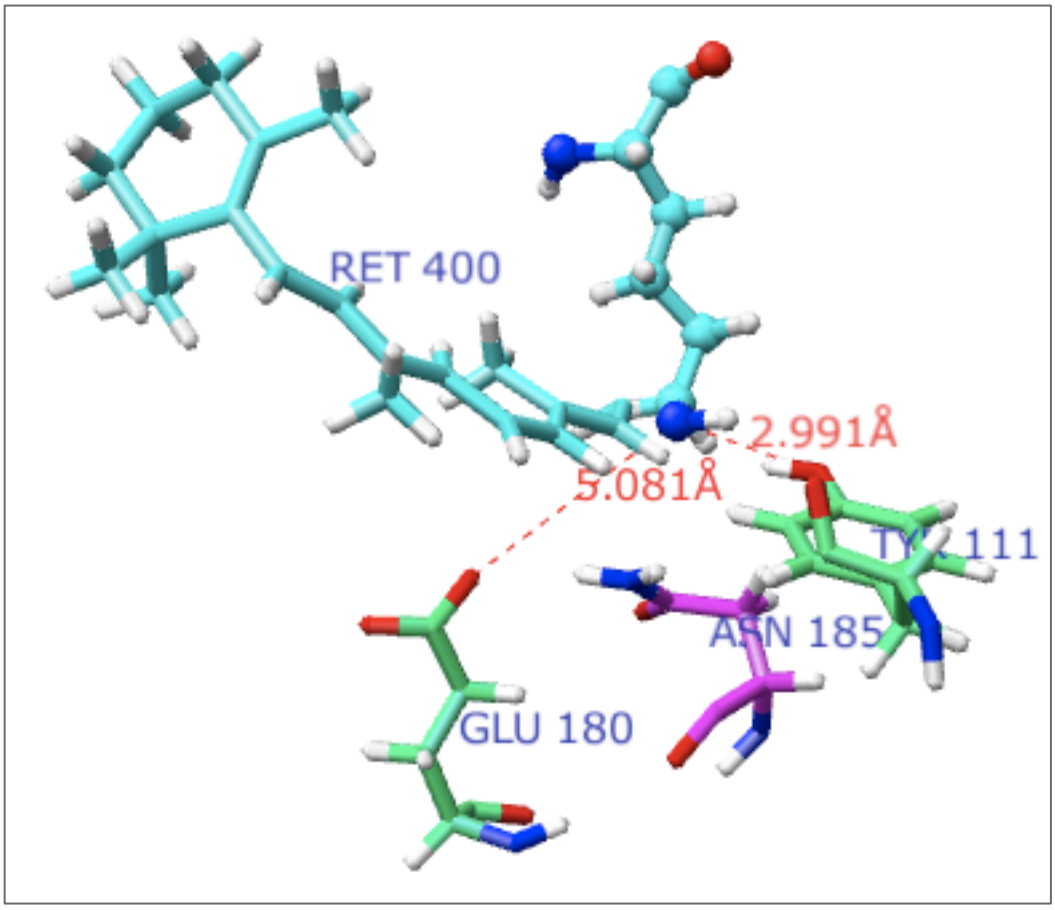

Figure 1.5 - Distances from protonated Schiff base nitrogen to side-chain oxygen of Glu180 (5.081 Å) and Tyr111 (2.991 Å).

While they could not assign the changes they observed to a particular tyrosine, through FTIR studies [56] Delange et al observed band changes in rhodopsin attributable to a tyrosinate vibrational mode, and concluded that one or more tyrosines participate in rhodopsin activation. On the other hand, Nakagawa et al [57] found that in octopus rhodopsin Tyr112 is neutral. Similarly, Herzfeld et al [58] found that between pH 2 and 10 all tyrosines in bacteriorhodpsion (bR) are protonated, and tyrosinate formation is not observed until pH 13, the point at which the protein begins to denature.

1.6 Squid Vision and Ocean Depth

Squid are one of four groups (along with cuttlefish, octopus, and chambered nautilus) that belong to the ocean dwelling Cephalopod species [59]. The high-resolution (2.5 Å) X-ray crystal structure of squid rhodopsin reported by Murakami et al [2] is that of the squid genre Todarodes pacificus, or Japanese Flying Squid. This genre is found in the Western Pacific, and in the Northern and Eastern Pacific as well, north and east from Japan to Canada [59].

When considering vision, the depth at which an ocean species inhabits is of importance because depth affects the prominence and intensity of atmospheric light that is transmitted through water, and the availability of light, in turn, affects species eye design [60] and the absorbance maximum of the visual pigment [61] [62] [63]. In ocean waters, downward irradiance of light has a maximum of between 480-500 nm at the surface,

and drops off toward 465 nm with increasing depth in clear ocean water [64]. Within the first 100 m of depth the orange-red part of the spectrum is almost entirely absorbed [60] (Figure 1.6).

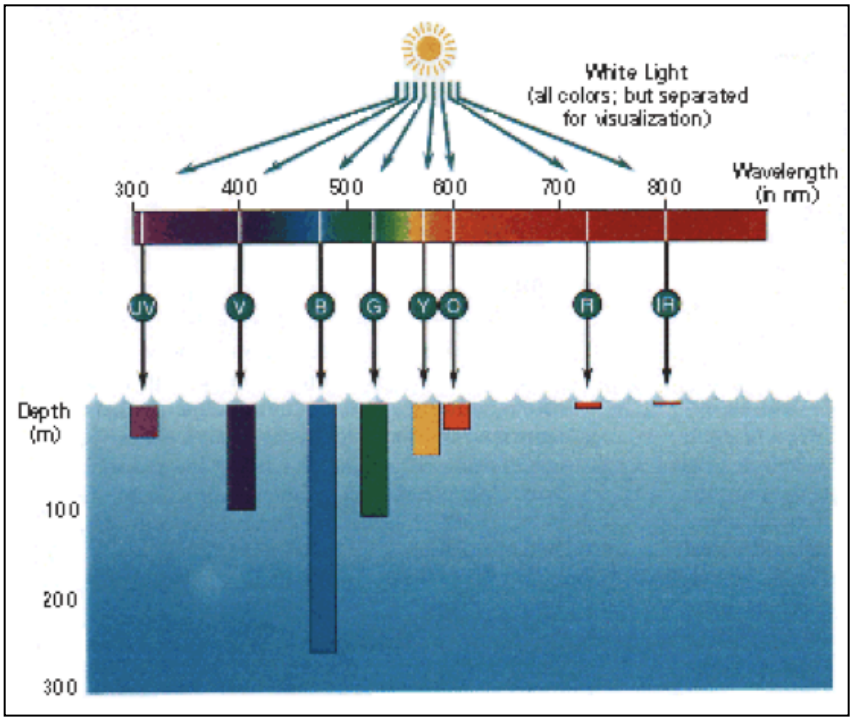

Figure 1.6 – Downward irradiance of light in ocean waters (image obtained from http://disc.sci.gsfc.nasa.gov/oceancolor/additional/science-focus/ocean-color/oceanblue.shtml)

Cephalopods are found from surface waters to over 5000 m in depth [59]. Morris et al compared the visual pigments of two squid species [65]; Alloteuthis subulata, a species that is found at a depth of about 200 m and has a rhodopsin absorption maximum of 499 nm; and Loligo forbesi, a species that is found at a depth of 360 m and has a rhodopsin absorption maximum of 494 nm. Morris et al found that replacement of a polar serine residue at site 270 in A. subulata rhodopsin, with that of a non-polar phenylanaline residue in L. forbesi rhodosin, appears to be responsible for the 5 nm

blue-shift in the absorption maximum of L. forbesi [65]. The deeper dwelling species, exposed to bluer wavelengths of light, has the molecular environment that provides a rhodopsin absorption maximum that is correspondingly blue-shifted when compared to the shallower dwelling species.

Todarodes pacificus can be found at even greater depths than A. subulata and L. forbesi. This species usually inhabits surface ocean waters to 100 m in depth, but can be found down to depths around 500 m [59]. In the coastal waters of Honshu Japan, schools of T. pacificus larger than 10 cm have been observed near the bottom of the continental shelf (~300-600 m depth) in the daytime [66]. As T. pacificus grow, they shift their distribution range from the temperate surface layer toward colder deeper layers [66]. In addition, T. pacificus has a rhodopsin absorption maximum of 480 nm [67] [68] [69] [70] blue-shifted from that of A. subulata and L. forbesi by 19 nm and 14 nm, respectively. The correlation beween visual pigment absorption and habitat depth seen with A. subulata and L. forbesi appears to hold for T. pacificus as well. In broadening our study to include three species of squid, Todarodes pacificus, Loligo forbesii, and Alloteuthis subulata, we attempted in this study to replicate the experimental rhodopsin absorption shifts observed between these species.

Chapter 2 – Methods

2.1 Computational Models

2.1.1 PDB File

The models used in this research are based on the rhodopsin crystal structure coordinates for the squid species Todarodes pacificus, solved at 2.5 Å resolution, deposited by Murakami and Kouyama in the Protein Data Bank (PDB) under the pdb accession number 2z73 [1, 2].

A pdb file presents molecular structure information derived from methods such as x-ray diffraction and NMR studies. The crystal structure for Todarodes pacificus was determined from x-ray diffraction methods. Using the x-ray diffraction method, a three dimensional structure of a crystallized molecule can be determined by scattering electrons in the protein crystal sample of interest with x-rays of wavelengths typically between 1-2 Å (high resolution). A map of the electron density within the crystal results, from which atomic coordinates can be interpreted [71]. Using these techniques, the first atomic resolution crystal structure of a membrane protein was published in 1985 [72, 73], the first high resolution x-ray structure of a G-Protein Coupled Receptor (GPCR) was reported in 2000 [72] [74], and the first Gq-coupled GPCR structure was determined in 2008, that of squid rhodopsin at 2.5 Å resolution [1, 2].

We used Monamer A of pdb file 2z73 as the starting point for our studies. The structure has 5682 atoms. In some models we manually added a water molecule to the photoreactive center, yielding a structure with 5685 atoms, and in some models we protonated the Glu180 residue as well, giving a total of 5686 atoms. In order to examine the spectral tuning effect of residues in various squid species, we also modified the residues Phe205 and Phe270 present in Todarodes pacificus in some models to represent the polar Tyr205 and/or Ser270 residues that are present in these same locations in the squid species Loligo forbesi (5683 atoms) and Alloteuthis subulata (5674 atoms).

2.1.2 XYZ Coordinate File

We converted the raw molecular information in pdb file 2z73 to an xyz coordinate format suitable for computational studies. To this end, we used TINKER molecular modeling software [73] [74] in conjunction with the force field Amber99 ('Amber' is an acronym for Assisted Model Building with Energy Refinement) [75] [76]. Amber is a molecular mechanical force field used for the simulation of biomolecules [77]. A force field is a combination of constants (from experimental data) and algebraic equations, approximating atoms as spheres and bonds as springs, and used to describe the potential energy of biomolecular systems.

Additional work was needed to complete the xyz coordinate files for our studies. While hydrogen atoms are abundant in protein structures, X-ray protein diffraction does not

detect these atoms because they are too light to contribute to diffraction [78]. Hydrogen atoms were thus added to our model using the utilities within the TINKER program. TiINKER software does not, however, recognize some non-standard residues such as the non-protein part of our model, retinal. Therefore when TINKER added hydrogens to the structure, retinal was overlooked in the process. To get around this issue we extracted retinal from the TINKER file, created a new retinal pdb file, and used the molecular modeling software Schroedinger and its interface, Maestro, to add hydrogen atoms to retinal [79]. This pdb file was then used to append the xyz file with hydrogenated retinal. Retinal was inserted into the xyz file with coordinates and protein attachment (Lys 305) appropriate for squid rhodopsin.

2.1.3 Modifications to Rhodopsin Model

To explore questions we have regarding the effect that surrounding residues have on the absorption properties of retinal, modifications were made to several of our models. Both the TINKER modeling utility and Gaussian's Gaussview graphical interface were used to make these modifications. Per our hypothesis that a water molecule is possibly missing from the pdf file structure of Todarodes pacificus in the vicinity of the photoreactive center, we inserted a water molecule into an available space near the residue Asn87 in some of our models. In questioning the assertion that Glu180 is negatively charged and acts as the counterion to the positively charged Schiff-base nitrogen in squid rhodopsin, we modified some of our models to include protonated

Glu180 instead of the standard deprotonated Glu180 that is used by the modeling software. And to examine the spectral tuning effect of residues in various squid species, we modified the residues Phe205 and Phe270 present in Todarodes pacificus to represent the polar Tyr205 and/or Ser270 residues that are present in these same locations in the squid species Loligo forbesi and Alloteuthis subulata.

2.2 ONIOM QM/MM Hybrid Method

In this study the computational ONIOM (**O**ur own **N**-layered **I**ntegrated molecular **O**rbital and molecular **M**echanics) method was used to investigate the Todarodes pacificus rhodopsin structure captured in pdb file 2z73, various modifications of the 2z73 structure, and the corresponding excitation energies of these molecular configurations. The goal in the optimization of a molecule such as rhodopsin is to solve for the lowest energy position, or optimized geometry, of the nuclei in that molecule. Force is exerted on nuclei when a change in position causes a change in energy. In computational studies, when the ratio of $\Delta_{energy}/\Delta_{position}$ or 'force' converges to zero, a stable geometry has been found [80]. To this end, the ONIOM method applies different levels of theory to different parts of a molecule to obtain the total energy of the system. The hybrid ONIOM QM/MM technique treats a small area of interest in a molecule at a computational expensive quantum mechanical (QM) level of theory and treats the rest of the molecule with a less expensive molecular mechanical (MM) method [81] [82]. By 'expensive' it is meant that more computational resources are needed to carry out calculations, such as

more time to execute mathematical operations, and more computing memory and storage to accommodate results [8]. Quantum mechanics treats molecules as collections of nuclei and electrons, using complex equations that describe the quantum state and behavior of particles, whereas molecular mechanics treats molecules as a collection of atoms and bonds, using simpler algebraic equations/classical mechanics laws, laws that often fail in describing very small masses and small transfers of energy [5] [6]. As such, quantum mechanics is the more appropriate level of theory to use for analyzing molecular regions [6] directly involved in reactions of the molecule [7]. However, since treating the entire system quantum mechanically is too computationally taxing, only a small area of interest in the molecule is usually treated at the QM level of theory and the rest of the system is treated at the less expensive MM level of theory [7]. The QM/MM technique and more general ONIOM method are incorporated in the Gaussian Program software that was employed in this study [4].

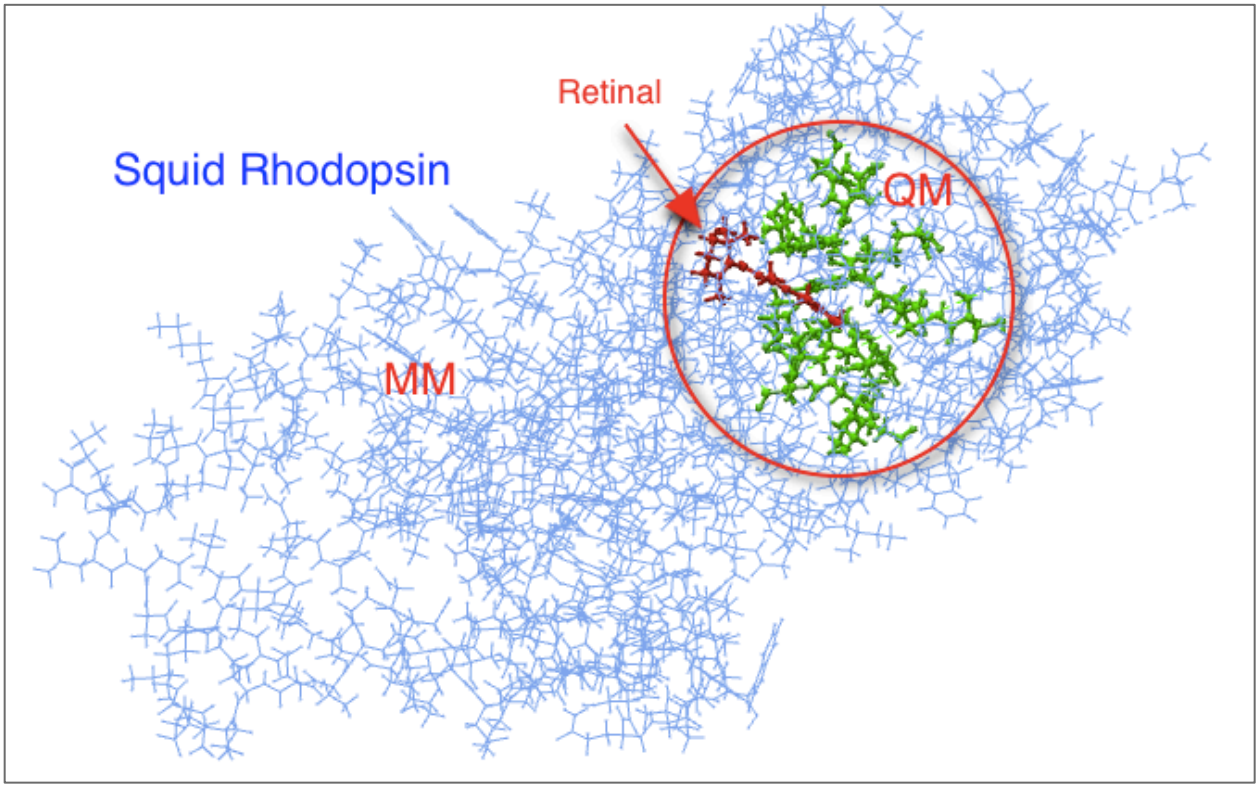

Figure 2.1 - Todarodes pacificus rhodopsin Model 9 partitioned into QM and MM regions.

Using the hybrid ONIOM QM/MM method, an area of chemical interest is partitioned off in the system by cutting covalent bonds and capping the resultant dangling bonds with 'link' atoms. Both the simplicity and the electronegativity value of hydrogen (close to that of carbon) make hydrogen the standard choice as link atom in biological systems [8], and therefore hydrogen was used to saturate the cut bonds in the current study. A layered model results with one layer consisting of the reduced area of interest, referred to as the 'QM region', and the second layer consisting of the remainder of the molecule, referred to as the 'MM region'. Figure 2.1 shows rhodopsin Model 9 from the current study partitioned in this manner.

The *total energy* of the system under study is determined by employing both the QM and MM levels of theory in three separate energy calculations, combined as follows:

$E_{total} = E_1 + E_2 – E_3$

E_1 is the energy of the *entire* system calculated using the MM level of theory,

E_2 is the energy of the partitioned area of interest (including the hydrogen link atoms) calculated using the QM level of theory, and

E_3 is the energy of the partitioned area calculated at the MM level of theory [7] [81] [82].

Without further modification, the above equation embodies the mechanical embedding (ME) scheme in that QM calculations on the reduced area are carried out in the absence of the rest of the molecule, and interactions *between* the layered regions are treated at the MM level of theory as expressed in the term E_1 [83]. In contrast, by employing an electronic embedding (EE) scheme, the above equation is modified so that terms E_2 and E_3 both include electrostatic interactions between the layered regions. Correspondingly, electrostatic interactions treated at the MM level of theory in terms E_1 and E_3 cancel each other out. Furthermore, the electrostatic interactions treated at the QM level of theory in term E_2 remain, resulting in the polarization of the reduced QM region by the surrounding protein environment [84] . Both schemes were used in the current study. While EE is clearly the best way of treating interactions between the

regions, switching between ME and EE allowed us to investigate the effect of polarization of the QM region due to neighboring charged and polar residues.

To avoid overpolarization of the QM region when using the EE scheme, default Gaussian scaling parameters were employed in this study. The default parameters turn off atom charges in the MM region within 2 bonds of the cut between the QM and MM regions, and the charges on the remaining atoms in the MM region remain unscaled.

Calculations were carried out using several different QM/MM partitioning arrangements of the Todarodes pacificus structure. The various QM regions used, defined by the residues contained within, are shown in the Table 2.1. Some of the QM regions include a water molecule in the QM region (indicated by -1W) and other QM regions do not include the addition of this water molecule (indicated by -0W). Figure 2.2 shows the residues in the QM region surrounding retinal in Model 9 of this study, the model in the current study with the largest defined QM region. The QM/MM partitioning arrangements used in the comparative analysis of the three squid species Todarodes pacificus, Loligo forbesi, and Alloteuthis subulata are shown in Table 2.2.

Table 2.1 – QM Regions used in Todarodes pacificus computational calculations

Model	*QM Region*
1-0W	Retinal (Ret)
2-0W	Ret, Asn87, Tyr111
3-0W	Ret, Asn87, Tyr111, Glu180
3-1W	Ret, Asn87, Tyr111, Glu180, Water
4-0W	Ret, Asn87, Tyr111, Glu180, Asn185, Cys186, Ser187
4-1W	Ret, Asn87, Tyr111, Glu180, Asn185, Cys186, Ser187, Water
5-0W	Ret, Val86, Asn87, Gly88, Tyr111, Glu180, Ala304, Lys305, Ala306
5-1W	Ret, Val86, Asn87, Gly88, Tyr111, Glu180, Ala304, Lys305, Ala306, Water
6-1W	Ret, Val86, Asn87, Gly88, Tyr111, Glu180, Cys184, Asn185, Cys186, Ser187, Ala304, Lys305, Ala306, Water
7-0W	Ret, Val86, Asn87, Gly88, Val110, Tyr111, Gly112, Phe113, Glu180, Cys184, Asn185, Cys186, Ser187, Ala304, Lys305, Ala306
8-0W	Ret, Val86, Asn87, Gly88, Val110, Tyr111, Gly112, Phe113, Tyr177, Glu180, Cys184, Asn185, Cys186, Ser187, Tyr277, Ala304, Lys305, Ala306
9-0W	Ret, Val86, Asn87, Gly88, Val110, Tyr111, Gly112, Phe113, Tyr177, Glu180, Cys184, Asn185, Cys186, Ser187, Phe188, Asp189, Tyr190, Tyr277, Ala304, Lys305, Ala306
9-1W	Ret, Val86, Asn87, Gly88, Val110, Tyr111, Gly112, Phe113, Tyr177, Glu180, Cys184, Asn185, Cys186, Ser187, Phe188, Asp189, Tyr190, Tyr277, Ala304, Lys305, Ala306, Water

Table 2.2 – QM Regions used in analysis of squid species

Species Model	*QM Region*
Todarodes pacificus	Ret, Ala304, Lys305, Ala306, Phe205, Phe270
Loligo fobesi	Ret, Ala304, Lys305, Ala306, Tyr205, Phe270
Alloteuthis subulata	Ret, Ala304, Lys305, Ala306, Tyr205, Ser270

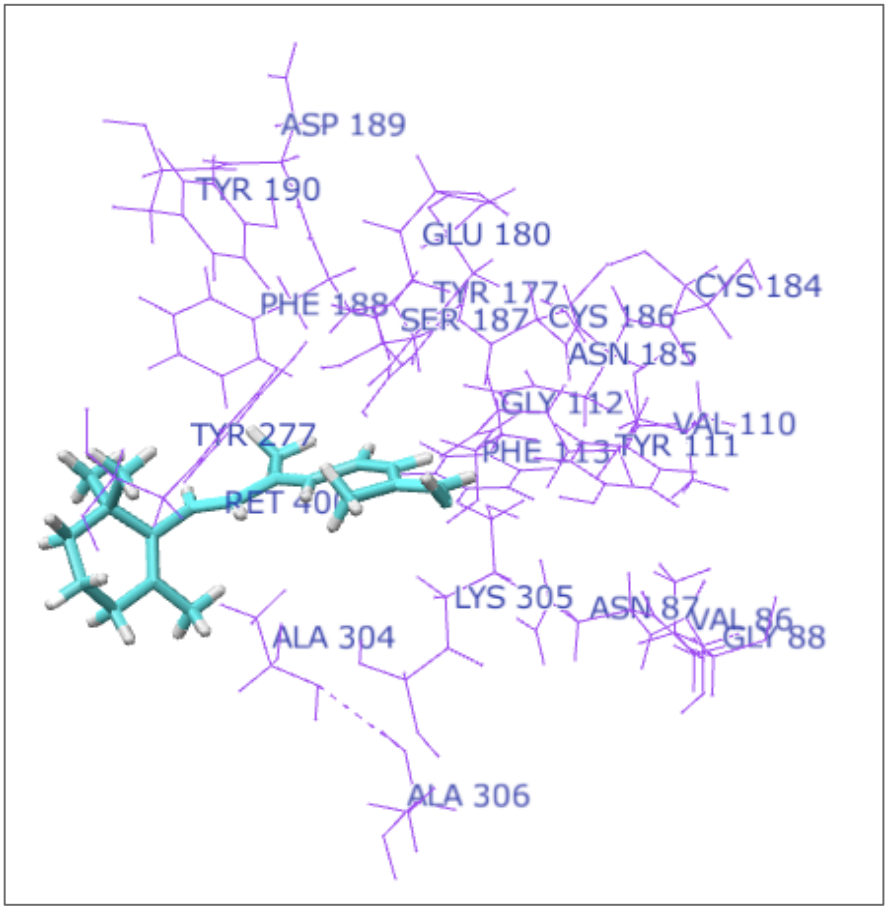

Figure 2.2– Residues (lavendar) included in QM region of Model 9 surrounding retinal (light blue)

2.3 Geometry Optimizations and Excitation Energy Calculations

Geometry optimizations were calculated first using the Hartree Fock ONIOM (hf/6-31g*:amber) level of theory, followed by the B3LYP hybrid density functional theory ONIOM (B3LYP/6-31g*:amber) level of theory. B3LYP is an acronym that stands for Becke, 3 parameter, Lee-Yang-Parr, which is an approximation for exchange energy in a DFT calculation. It is a Hartree-Fock exchange integral that is evaluated with Kohn-Sham orbitals which are functionals of density [10]. Because both HF and DFT are

incorporated in the method, B3LYP belongs to the class of 'hybrid' functionals, and is one of the most popular methods in this category [8]. The terminology 6-31g* stands for a basis set that is used with the DFT method, incorporating 6 gaussian type orbitals (GTOs) used for inner shell electrons, 3 GTOs for inner valance, and 1GTO for outer valence electrons. The asterisk indicates that d-type functionals are added on to atoms, allowing the polarization of atomic orbitals and thus a better approximation of the system. During geometry optimizations, a constraint was put on the alpha carbons of those residues within the MM region, freezing their movement while allowing the attached side chains to optimize. Excitation energies were calculated using the B3LYP hybrid td-dft ONIOM (B3LYP td=(Nstates)/6-31g*:amber) level of theory.

Chapter 3 – Results and Discussion

3.1 Water Molecule in Photoreactive Center

The results in Table 3.1 were obtained by performing initial geometry optimizations on two models of Todarodes Pacificus rhodopsin, the models differing by the number of residues included in the quantum region. Model 1 contains only retinal in the quantum region, and Model 2 contains retinal, Asn87 and Tyr111. In both of the optimized structures, it was observed that the distance between the amide oxygen of the Asparagine-87 (Asn87) side chain and the retinal Schiff base nitrogen was approximately 1 Å shorter than the distance between those same atoms in the experimental xray structure from pdb file 2z73.

Table 3.1 – Initial geometry optimization of Todarodes pacificus rhodopsin: Resultant distance between amide oxygen of Asn87 side chain and retinal Schiff base nitrogen

Model	*Distance (Å) Asn87 – Ret N*	*Residues in Quantum Region*
Experimental pdb 2z73	3.73	
Model 1	2.91	Retinal
Δ from Exp	*-0.82*	
Model 2	2.78	Retinal, Asn87, Tyr111
Δ from Exp	*-0.95*	

From these results it was hypothesized that the x-ray structure may be missing a water molecule in the photoreactive center, and upon optimization, the oxygen and nitrogen atoms referenced moved into available spaces in lower energy positions, shortening the interatomic distance noted.

A water molecule was therefore inserted into the rhodopsin model in an available space in the vicinity of retinal and Asn87 (see Figure 1.4). Upon optimization after this addition, it was observed that inserting a water molecule indeed brought the distance between the Asn87 oxygen and retinal nitrogen much closer to the experimental value. However, this improvement was observed only when a certain defined quantum region was employed in the optimization calculation. In additional calculations, when the *only* variable changed in a model was expansion of the quantum region to include additional residues (with or *without* the addition of a water molecule), distances between residues varied as well, including that between Asn87 and retinal. The addition of a water molecule to the QM region *in conjunction* with an expanded quantum region led to a distance between Asn87 and retinal, in some models, that *exceeded* the experimentally determined distance. Table 3.2 shows the independent impact that the quantum region size, and the addition of a water molecule to the photoreactive center, both have on the calculated distances and molecular absorbances of Todarodes Pacificus rhodopsin. We focused attention on three distances (Figure 3.1), the distance between retinal's Schiff Base nitrogen and: (1) the amide oxygen of the Asn87 side chain; (2) the hydroxyl oxygen of Tyr111; and (3) the carboxylic acid oxygen of Glu180. The residues Glu180 and Tyr111 were of particular interest due to their proximity and potential stabilizing effects on the positive charge of the protonated Schiff base.

Table 3.2 - Impact of (1) quantum region size and of (2) addition of water molecule to photoreactive center on interatomic distances and molecular absorbance in Todarodes pacificus. Electronic embedding employed / Glu180 is unprotonated.

	Distance (Å)						*Absorbance (nm)*	
	Distance A: N-Asn87		*Distance B: N-Tyr111*		*Distance C: N-Glu180*			
Model	*0W*	*1W*	*0W*	*1W*	*0W*	*1W*	*0W*	*1W*
1	2.91	-	3.19	-	4.94	-	518.54	-
Δ	*-0.82*		*+0.20*		*-0.14*		*+39*	
2	2.80	-	3.60**	-	4.85	-	488.79	-
Δ	*-0.93*		*+0.61*		*-0.23*		*+8.8*	
3	2.86	3.67	3.17	3.01	4.39	4.36	473.00	471.30
Δ	*-0.87*	*-0.06*	*+0.18*	*+0.02*	*-0.69*	*-0.72*	*-7.0*	*-8.7*
4	2.82	3.42	3.23	3.10	4.58	4.57	468.43	467.24
Δ	*-0.91*	*-0.31*	*+0.24*	*+0.11*	*-0.50*	*-0.51*	*-12*	*-13*
5	3.04	4.50	3.14	3.19	4.43	4.48	493.74	491.62
Δ	*-0.69*	*+0.77*	*+0.15*	*+0.20*	*-0.65*	*-0.60*	*+14*	*+12*
6	-	4.50	-	3.20	-	4.56	494.66	-
Δ		*+0.77*		*+0.21*		*-0.52*	*+15*	
7	3.72	-	2.99	-	4.55	-	524.14	-
Δ	*-0.01*		*0.00*		*-0.53*		*+44*	
8	3.78	-	2.99	-	4.68	-	526.70	-
Δ	*+0.05*		*0.00*		*-0.40*		*+47*	
9	2.80	4.47	3.07	2.96	5.34	5.23	NA	NA
Δ	*-0.93*	*+0.74*	*+0.08*	*-0.03*	*+0.26*	*+0.15*		
Exp	***3.73***		***2.99***		***5.08***		***480***	
Δ%	35	32	8.0	8.1	22	20	12	5.9

- Models are defined by quantum region contents. Models are cross-referenced to a QM region containing an inserted water molecule near retinal (1W), or to a QM region not containing this additional water molecule (0W). **Residues in QM Region** are as follows. Note (p) = indicates residue is polar, (-) = indicates residue has a negative charged side-chain, (+) = indicates residue has a positive charged side- chain:
  Model 1 = Retinal (ret)
  Model 2 = Ret, Asn87 (p), Tyr111 (p)
  Model 3 = Model 2 residues, and Glu180 (-)
  Model 4 = Model 3 residues, and Asn185 (p), Cys186 (p), Ser187 (p)
  Model 5 = Model 3 residues, and Val86, Gly88, Ala304, Lys305 (+), Ala306
  Model 6 = Model 5 residues, and Cys184 (p), Asn185 (p), Cys186 (p), Ser187 (p)
  Model 7 = Model 6 residues, and Val110, Gly112, Phe113
  Model 8 = Model 7 residues, and Tyr177 (p), Tyr277 (p)
  Model 9 = Model 8 residues, and Phe188, Asp189 (+), Tyr190 (p)
- ***Experimental*** distances referenced are from x-ray data set PDB file 2Z73, monomer A, resolved at 2.5 Å [2].
- ***Experimental*** Absorbance of 480 nm references: [55] [67] [68] [70] [85]
- **Distances** are defined as follows:

A= Distance (Å) between Schiff Base N of retinal and Amide O of Asn87 side chain
B= Distance (Å) between Schiff Base N of retinal and Hydroxyl O of Tyr111
C= Distance (Å) between Schiff Base N of retinal and Carboxylic Acid O of Glu180

- Δ = Difference from experimental value
- Δ% = percent change of given distance or absorbance over all models tested
- ** Results for Model 2-0W = outlier value.

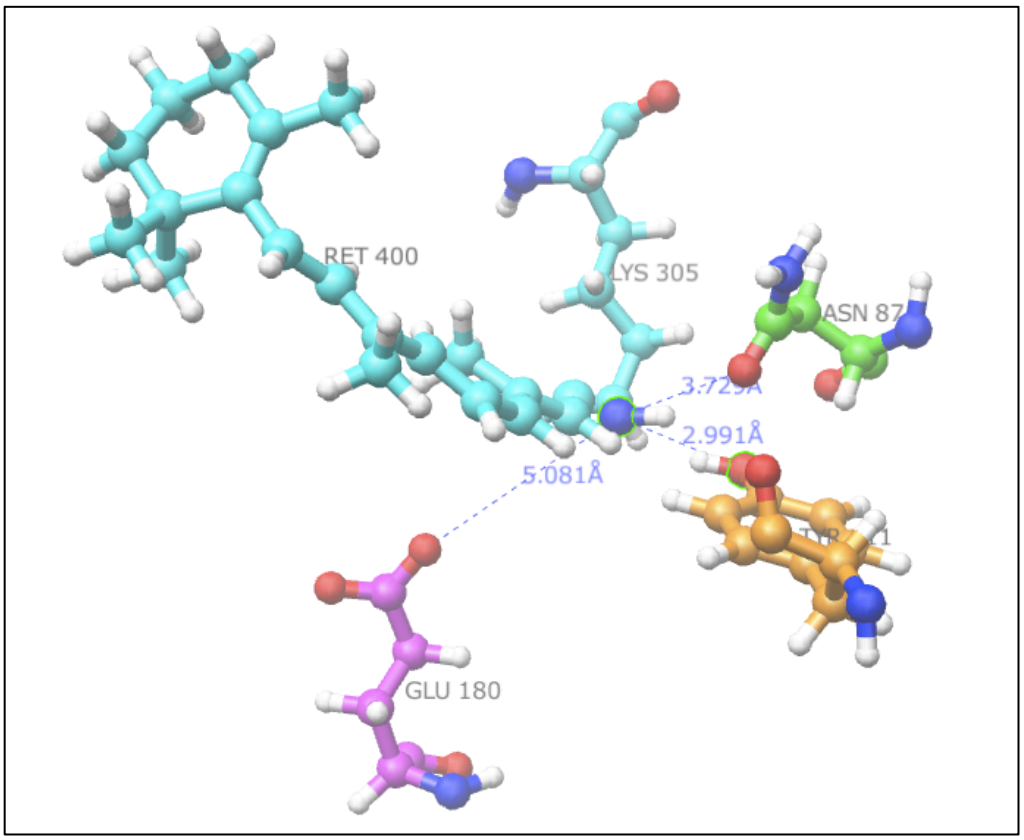

Figure 3.1 – Distances between Schiff base nitrogen and: amide oxygen of the Asn87 (3.73A); hydroxyl oxygen of Tyr111 (2.99A); and carboxylic acid oxygen of Glu180 (5.08A).

Residues incrementally added to the quantum region of the various models are residues within approximately 5 Å of the chromophore retinal, or are attached to residues of interest that are within 5 Å of retinal. Residues of particular interest are those with polar or charged side-chains that may help 'tune' the absorbance spectrum of rhodopsin. A positive charge is spread along the conjugated chromophore system of retinal as a result of the protonated Schiff base between retinal and Lys305. Negatively charged or polar residues surrounding retinal may stabilize this positive charge, thereby lowering the energy of the transition from the ground to first excited state, and accordingly

shifting the absorption of the molecule to a longer wavelength [86]. Cuts made to separate the QM region from the MM region were made to peptide bonds between residues, with resultant dangling bonds in the QM region capped with hydrogen atoms. Some additional residues, beyond those of interest, were included in the quantum region of some models so that the boundary between the QM and MM region was pushed farther away from the chromophore and residues of interest. Solt et al. found that results of QM/MM calculations are affected by the definition of the quantum region, and that the average force errors in the polar region of interest decreased with increasing size of the QM region, reaching an acceptable level only when the QM region included at least 500 atoms, and the radius of the QM region from the area of interest approached 9 Å [87]. The intent in the current study was to include all residues within 9 Å of retinal (Figure 3.2), however computational resource limits were reached well before that goal. Calculations including only a limited number of the residues within 5 Å (Figure 3.3) of retinal took several weeks to complete. The excitation energy calculation for Model 9 did not complete successfully due to the computational expense of the calculation. The current study thus included QM regions containing at most 20 residues (297 atoms) surrounding retinal, in addition to a water molecule added near the chromophore, as observed in Models 1- 9.

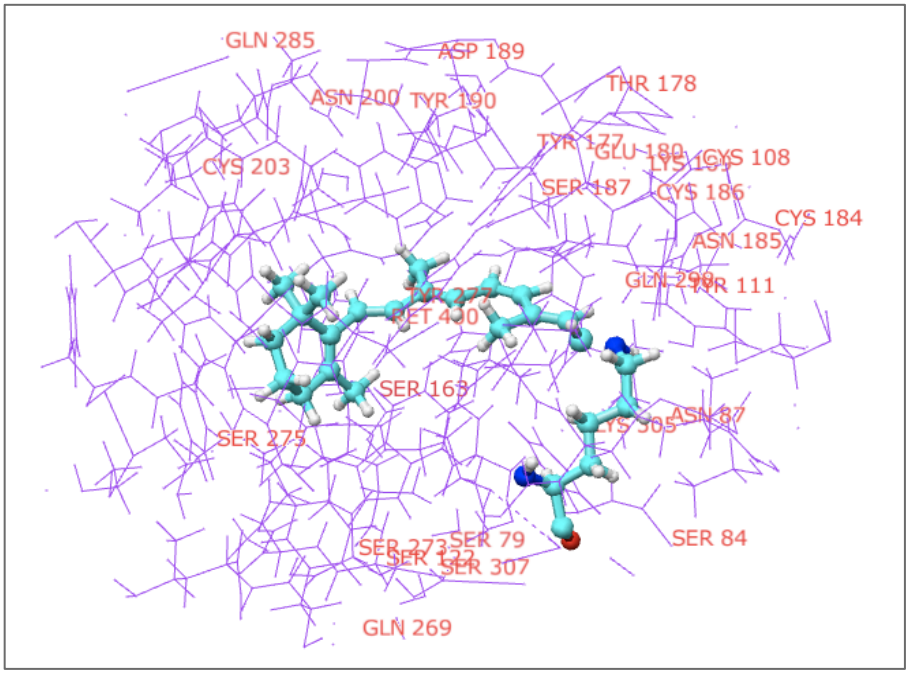

Figure 3.2– All residues (lavender wires) within 9 Å of retinal (bright blue). Polar, acidic, and basic residues are labeled. Schiff base nitrogen (royal blue) is between retinal and Lys305.

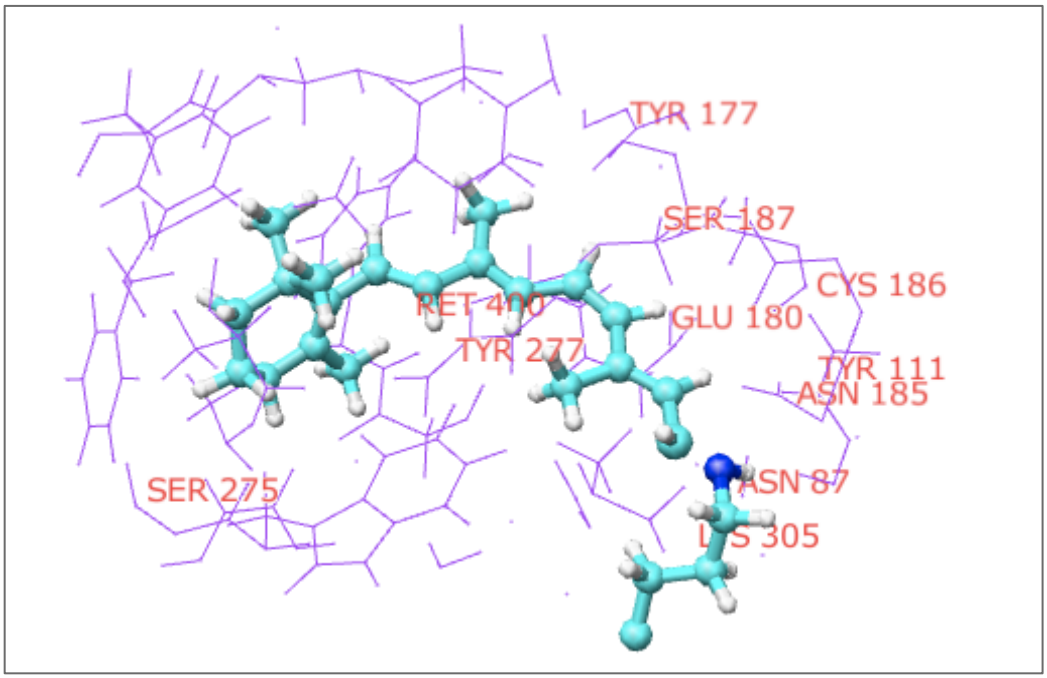

Figure 3.3 – All residues (lavender wires) within 5 Å of retinal (bright blue). Polar, acidic, and basic residues are labeled. Schiff base nitrogen (royal blue) is between retinal and Lys305.

Table 3.2 results show that as the *size of the quantum region is increased* (i.e. the number of residues included in the quantum region is increased) both the interatomic distances under observation and the molecular absorbances change between models. This observation holds for models that have a water molecule inserted into the photoreactive area, and models that do not have the addition of this water. Table 3.2 also shows that *the addition of a water molecule to the photoreactive center* impacts the interatomic distances under observation, particularly with respect to distance A, but does not have a significant impact on molecular absorbance.

It is difficult to draw the conclusion that the x-ray structure presented in pdb file 2z73 is missing a water molecule in the photoreactive center. The addition of a water molecule to Model 3 does improve the distance between the side chain amide oxygen of Asn87 and retinal's Schiff base nitrogen. However results for Model 7, in which an additional water molecule in <u>not</u> present, suggest the best model emerges from that with a medium size QM region, casting doubt on previous suggestions and our earlier calculations that propose a water is present. Optimization calculations on models with QM regions *larger* than that included in Model 7 yield distances that begin to worsen and exceed experimental values, as seen in Model 9. A possible explanation for this has to do with the fact that adding more residues in the QM region adds extra boundaries that may create overpolarization effects.

3.2 Glu180 as Counterion

As previously noted, residues in the protein environment with polar or charged side-chains can stabilize the delocalized positive charge that exists along retinal's conjugated π electron system, lowering the transition state energy and red-shifting the absorption spectrum [86]. In contrast, a negative counterion located near the protonated Schiff base serves to *localize* the positive charge of the Schiff base [88], raising the transition state energy and leading to a blue-shift of the molecule's absorbtion. To explore the purported role of Glu180 as the counterion in squid rhodopsin two models (both with and without addition of water to the active center) were altered by protonating Glu180, followed by carrying out optimization and excited state calculations in order to observe the impact of these structural modifications. Table 3.3 shows results of calculations that employed electronic embedding, and Tale 3.4 shows results of calculations that employed mechanical embedding.

Of note in both experiments is the marked increase in absorbance for both Model 3 and Model 4 when Glu180 is protonated. When electronic embedding is employed (Table 3.3) there is a 9-10% increase in absorbance for both models, regardless of the addition of a water molecule to the photoreactive center, causing a red-shift of between 43 and 46 nm. When mechanical embedding is used (Table 3.4) there is a 12-16% increase in absorbance over both models, the addition of a water molecule again not markedly affecting absorbance, and a resultant red-shift of 60-77 nm. These results support findings that Glu180, in its unprotonated state, acts as a counterion to rhodopsin,

localizing the positive charge on the Schiff base between retinal and Lys305. When that function is removed via protonation of Glu180, a notable red-shift is observed, indicating delocalization of the positive charge that results from the protonated Schiff base.

Table 3.3 - Impact of protonation of Glu180 on models 3 and 4 (electronic embedding employed).

	Distance (Å)						*Absorbance (nm)*	
	Distance A: N-Asn87		*Distance B: N-Tyr111*		*Distance C: N-Glu180*			
Model	*0W*	*1W*	*0W*	*1W*	*0W*	*1W*	*0W*	*1W*
3U	2.86	3.67	3.17	3.01	4.39	4.36	473.00	471.30
Δ	*-0.87*	*-0.06*	*+0.18*	*+0.02*	*-0.69*	*-0.72*	*-7.0*	*-8.7*
3P	2.77	3.42	3.17	3.00	5.13	5.01	519.03	515.16
Δ	*-0.96*	*-0.31*	*+0.18*	*+0.01*	*+0.05*	*-0.07*	*+39*	*+35*
V	*-0.09*	*-0.25*	*0.00*	*-0.01*	*+0.74*	*+0.65*	*+46*	*+44*
V%	*-3.1*	*-6.8*	*0.0*	*-0.33*	*+17*	*+15*	*+9.7*	*+9.3*
4U	2.82	3.42	3.23	3.10	4.58	4.57	468.43	467.24
Δ	*-0.91*	*-0.31*	*+0.24*	*+0.11*	*-0.50*	*-0.51*	*-12*	*-13*
4P	2.74	3.09	3.22	3.12	5.40	5.35	514.09	509.93
Δ	*-0.99*	*-0.64*	*+0.23*	*+0.13*	*+0.32*	*+0.27*	*+34*	*+30*
V	*-0.08*	*-0.33*	*-0.01*	*+0.02*	*+0.82*	*+0.78*	*+46*	*+43*
V%	*-2.8*	*-9.6*	*-0.31*	*+0.65*	*+18*	*+17*	*+9.7*	*+9.1*
Exp	***3.73***			***2.99***			***5.08***	

- Models are defined by quantum region contents. Models are cross-referenced to a QM region containing an inserted water molecule near retinal (1W), or to a QM region not containing this additional water molecule (0W). **Residues in QM Region** are as follows. Note (p) = indicates residue is polar, (-) = indicates residue has a negative charged side-chain, (+) = indicates residue has a positive charged side- chain:
  Model 3 = Ret, Asn87 (p), Tyr111 (p), Glu180 (-)
  Model 4 = Ret, Asn87 (p), Tyr111 (p), Glu180 (-), Asn185 (p), Cys186 (p), Ser187 (p)
- ***Experimental*** distances referenced are from x-ray data set PDB file 2Z73, monomer A, resolved at 2.5 Å [2].
- ***Experimental*** Absorbance of 480 nm references: [55] [67] [68] [70] [85]
- **Distances** are defined as follows:

A= Distance (Å) between Schiff Base N of retinal and Amide O of Asn87 side chain
B= Distance (Å) between Schiff Base N of retinal and Hydroxyl O of Tyr111
C= Distance (Å) between Schiff Base N of retinal and Carboxylic Acid O of Glu180

- U=Glu180 is unprotonated in given model
- P=Glu180 is protonated in given model
- Δ = Difference from experimental value
- V= variance between models for given measure
- V% = percent change between models for given measure

Table 3.4 - Impact of protonation of Glu180 on models 3 and 4 (mechanical embedding employed).

	Distance (Å)						*Absorbance (nm)*	
	Distance A: N-Asn87		*Distance B: N-Tyr111*		*Distance C: N-Glu180*			
Model	*0W*	*1W*	*0W*	*1W*	*0W*	*1W*	*0W*	*1W*
3U	2.95	3.88	3.11	3.00	4.26	4.18	474.18	468.94
Δ	*-0.78*	*+0.15*	*+0.12*	*+0.01*	*-0.82*	*-0.90*	*-5.8*	*-11*
3P	2.82	3.63	3.11	2.95	5.09	4.93	551.08	544.37
Δ	*-0.91*	*-0.10*	*+0.12*	*-0.04*	*+0.01*	*-0.15*	*+71*	*+64*
V	*-0.13*	*-0.25*	*0.00*	*-0.05*	*+0.83*	*+0.75*	*+77*	*+75*
V%	*-4.4*	*-6.4*	*0.0*	*-1.7*	*+19*	*+18*	*+16*	*+16*
4U	2.92	3.86	3.17	3.05	4.39	4.31	487.86	480.36
Δ	*-0.81*	*+0.13*	*+0.18*	*+0.06*	*-0.69*	*-0.77*	*+7.9*	*+0.36*
4P	2.82	3.58	3.16	2.98	5.34	5.21	548.09	542.73
Δ	*-0.91*	*-0.15*	*+0.17*	*-0.01*	*+0.26*	*+0.13*	*+68*	*+63*
V	*-0.10*	*-0.28*	*-0.01*	*-0.07*	*+0.95*	*+0.90*	*+60*	*+62*
V%	*-3.4*	*-7.3*	*-0.32*	*-2.3*	*+22*	*+21*	*+12*	*+13*
Exp	***3.73***			***2.99***			***5.08***	

- Models are defined by quantum region contents. Models are cross-referenced to a QM region containing an inserted water molecule near retinal (1W), or to a QM region not containing this additional water molecule (0W). **Residues in QM Region** are as follows. Note (p) = indicates residue is polar, (-) = indicates residue has a negative charged side-chain, (+) = indicates residue has a positive charged side- chain:
  Model 3 = Ret, Asn87 (p), Tyr111 (p), Glu180 (-)
  Model 4 = Ret, Asn87 (p), Tyr111 (p), Glu180 (-), Asn185 (p), Cys186 (p), Ser187 (p)
- ***Experimental*** distances referenced are from x-ray data set PDB file 2Z73, monomer A, resolved at 2.5 Å [2].
- ***Experimental*** Absorbance of 480 nm references: [55] [67] [68] [70] [85]
- **Distances** are defined as follows:

A= Distance (Å) between Schiff Base N of retinal and Amide O of Asn87 side chain
B= Distance (Å) between Schiff Base N of retinal and Hydroxyl O of Tyr111
C= Distance (Å) between Schiff Base N of retinal and Carboxylic Acid O of Glu180

- U=Glu180 is unprotonated in given model
- P=Glu180 is protonated in given model
- Δ = Difference from experimental value
- V= variance between models for given measure
- V% = percent change between models for given measure

Of note in this experiment is the difference between absorbance results obtained with use of electronic embedding (EE) vs. mechanical embedding (ME). Table 3.4 (ME method) shows that absorbances are notably more red-shifted when Glu180 is protonated, in comparison to results obtained through use of EE, shown in Table 3.3.

Both ME and EE calculations show that the protein's absorbance is red-shifted when Glu180 is protonated, reflecting removal of the localizing effect of Glu180 on the positive charge of the Schiff base nitrogen. When using EE, the QM region "sees" polar residues in the protein environment that can moderate the effect of Glu180 on the Schiff base nitrogen. When using ME, the impact of the protein environment is *not* included in the energy calculation, there is no moderation to Glu180's effect, and thus the red-shift observed upon protonation of Glu180 is greater than when using the EE scheme.

As shown in Tables 3.3 and 3.4, protonation of Glu180 also leads to an appreciable change in the distance between the Schiff Base nitrogen and the carboxylic acid oxygen of Glu180. When electronic embedding is employed, there is a 15-18% increase (an increase of 0.65-0.82 Å) in this distance over both models, the addition of a water molecule to the photoreactive center not having a significant impact on this result. When mechanical embedding is used, there is a corresponding increase of 18-22% (an increase of 0.75-0.95 Å). These results further suggest that an unprotonated Glu180 acts as a counterion to the protonated Schiff base, its negative charge interacting with and stabilizing the positive charge on the Schiff base, resulting in a shortened distance between the two atoms.

A separate QM/MM experiment was carried out to explore the contribution that each protein residue has on rhodopsin's absorbance wavelength. The charge on each residue was sequentially turned off, with the change in absorbance energy recorded as

each residue's charge was zeroed. Figure 3.4 shows that when the charge on Glu180 is turned off, there is a red-shift in absorbance of nearly 70 nm, again substantiating the role of Glu180 as counterion. This result reinforces the results in Tables 3.3 and 3.4 that show a significant red-shift in absorbance when Glu180 is protonated -- in essence when the charge on Glu180 is 'turned off'. The results of this experiment show as well the effect that several *additional* amino acids have on the spectral tuning of the chromophore. With their charges turned on, the polar Asn87 and Tyr111 amino acids contribute a blue-shift of approximately 20 and 10 nm, respectively, to the absorbance spectrum of rhodopsin. The charges of Asn185 and Gly115 contribute a red-shift of approximately 15-20 nm. The results also show that several additional protein residues

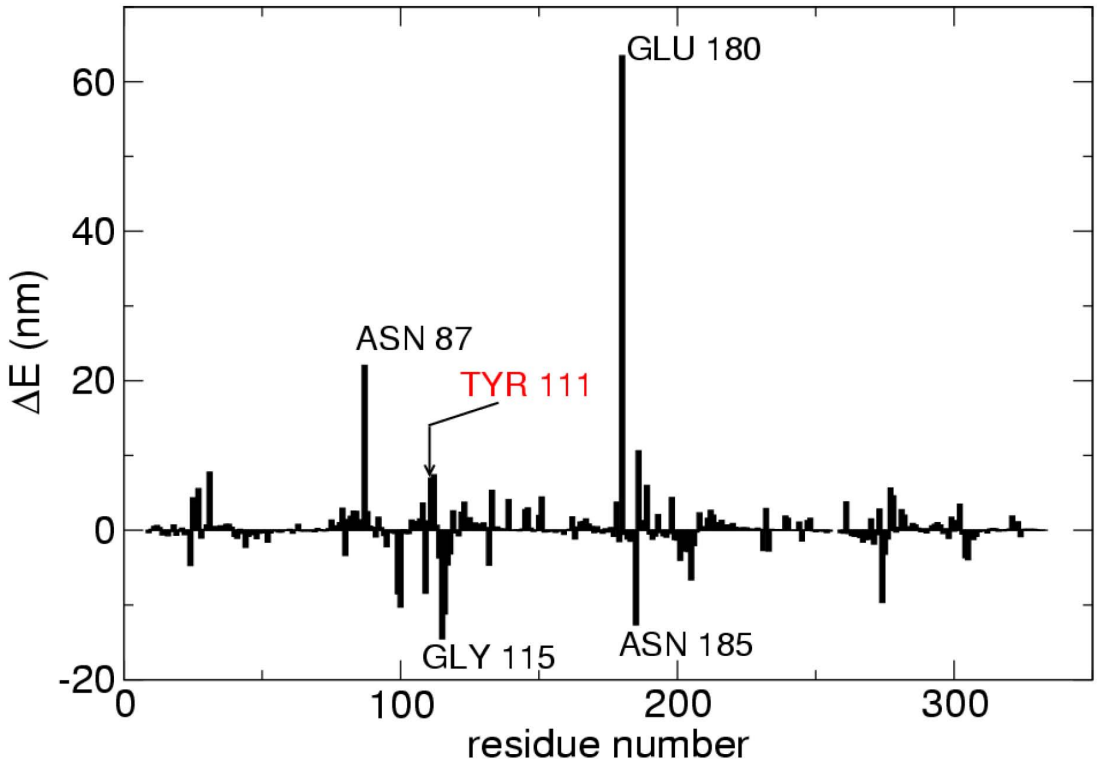

Figure 3.4 – Contribution of residues in Todarodes pacificus rhodopsin to absorption wavelength.

combine to provide retinal with a background environment of various polarities/charges that help shape the absorbance spectrum of the chromophore and molecule.

3.3 Comparison of Absorbance in Squid Species

Two amino acids in the Todarodes pacificus rhodopsin model that are in close proximity to the chromophore (within 5 Å, Figure 3.5) were modified to simulate residues in other species of squid. The squid species Alloteuthis subulata contains a polar serine residue, Ser270, at the 270 site in rhodopsin. At that same site, the squid species Loligo forbesi contains the non-polar Phe270, as does Todarodes pacificus. As well, the species Alloteuthis subulata contains a polar tyrosine residue, Tyr205, at the 205 site in rhodopsin. Loligo forbesi also contains Tyr205 at this site, but Todarodes pacificus contains the non-polar Phe205.

Morris et al found that replacement of the polar serine residue at site 270 in Alloteuthis subulata rhodopsin, with that of a non-polar phenylanaline residue in Loligo forbesi rhodosin, is responsible for a 5 nm blue-shift in the absorption maximum of Loligo forbesi [65]. The experimentally determined absorption maximum of Todardoes pacificus rhodopsin is 480 nm, blue-shifted 14 nm from that of Loligo forbesi rhodopsin. In the current study, it was hypothesized that if these two key residues in Todarodes pacificus, located at sites 270 and 205, were converted to Tyr205 and Ser270, QM/MM

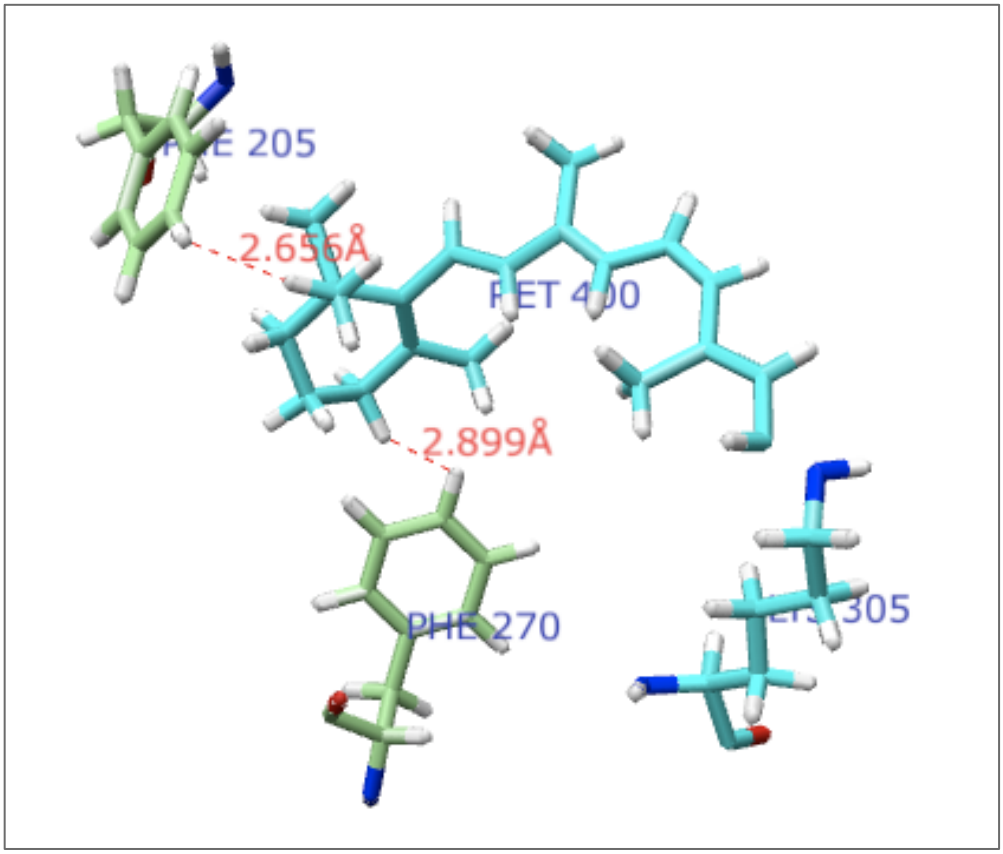

Figure 3.5 – Location of Todarodes pacificus residues Phe205 (2.656 Å from Ret), and Phe270 (2.899 Å from Ret)

excitation energy calculations would be able to produce the experimental energies of Loligo forbesi and Alloteuthis subulata. As shown in previous experiments in this study concerning a water molecule added to the QM region, the reliability of the QM/MM method in reproducing accurate rhodopsin absorbance energies is questionable, as results varied when the definition of the QM region was varied. This can be seen in the current experiment as well, as calculated absorbance energies for the three squid species are 10-11% higher than experimental values. However, what is relevant is that

the QM/MM method, while inaccurate in predicting absolute energy values, was able to reproduce the shifts in absorption energies that are seen between experimental values.

The software program Gaussian [4] and its graphical interface Gaussview were used to first convert Phe205 in Todarodes pacificus rhodopsin to a Tyr205 residue, as is found in Loligo forbesi. Next, in addition to the altered Phe205, the residue Phe270 was converted to Ser270, as is found in Alloteuthis subulata. Table 3.5 shows that excitation energy calculations performed on the Todarodes pacificus model yielded an absorption energy of 534 nm. Calculations on the Loligo forbesi model returned an absorbance energy of 549 nm, a 15 nm red-shift from that of Todarodes pacificus, which is in good agreement with the 14 nm red-shift seen in experimental data. Excitation energy calculations performed on the Alloteuthis subulata model generated an excitation energy of 556 nm, a 7 nm red-shift from that of Loligo forbesi, which is again proximate to the 5 nm red-shift shown in experimental data.

Table 3.5 - Absorbance of Todarodes pacificus rhodopsin compared to absorbance in Todarodes pacificus rhodopsin models that have been modified with residues specific to Loligo forbesi and Allotheuthis subulata rhodopsin

	Todarodes pacificus	*Loligo forbesi*	*Alloteuthis subulata*
Residues included in Quantum Region	Ret, Ala304, Lys305, Ala306, Phe205, Phe270	Ret, Ala304, Lys305, Ala306, Tyr205, Phe270	Ret, Ala304, Lys305, Ala306, Tyr205, Ser270
Experimental Abs (nm)	480	494	499
Shift from Todarodes pacificus (nm)		+14	+5
Observed Abs (nm)	534.33	549.29	556.21
Shift from Todarodes pacificus (nm)		+14.96	+6.92

What is also interesting about these results is that they provide an example of how polar residues in proximity to retinal can help stabilize the delocalized positive charge along the chromophore, leading to a red-shift in the absorption spectrum. The sequential modification of two non-polar residues in Todarodes pacificus to polar residues led to an incremental shift of the absorbance in the direction and magnitude that is expected.

Chapter 4 – Concluding Remarks

In trying to determine if a water molecule exists near the chromophore in Todardoes pacificus rhodopsin (not present in the molecule's pdb file), a water molecule was inserted into the rhodopsin model, and optimization and excited state calculations were carried out. It was found that insertion of a water molecule does not have a significant impact on absorbance calculations, yet it indeed influences the geometry of the molecule, in some models improving the inter-residue distances towards experimental values. The addition of a water molecule to Model 3 improved the distance between the side chain amide oxygen of Asn87 and retinal's Schiff base nitrogen.

However, at the same time, it was observed that the definition of the quantum region impacts the distances between residues as well, and also influences the absorbance calculations. Results for Model 7, in which an additional water molecule in *not* present, suggest the best model emerges from that with a medium size QM region (approximately 5 Å radius), casting doubt on previous suggestions and our earlier calculations that propose a water is present. Optimization calculations on models with QM regions *larger* than that included in Model 7 yield distances that begin to worsen and exceed experimental values, as seen in Model 9. A possible explanation for this is that adding more residues in the QM region adds extra boundaries that may create overpolarization effects.

There are several published journel articles that discuss possible issues that could be encounterd with application of the QM/MM method in analysis of biological molecules such as rhodopsin. Analysis of these issues is beyond the scope of the current study, but are nonetheless important to acknowledge and consider for future studies. As commented on previously, Solt et al found that results of QM/MM calculations are affected by the definition of the quantum region, and that the average force errors in the polar region of interest decreased with increasing size of the QM region, reaching an acceptable level only when the QM region included at least 500 atoms, and the radius of the QM region from the area of interest approached 9Å [87]. Wanko et al [89] discuss the high sensitivity of absorption energies on the ground-state structure of retinal, which is itself very sensitive to the method used for geometry optimizations. They examine electrostatic and mechanical influences that the protein environment may have on retinal, a chromophore with high polarizability and structural flexibility, and also discuss, in contrast, the strong changes in the electric dipole moment of retinal, which may itself induce significant polarization of the protein environment. These matters are important in QM/MM applications where the active site is partitioned from the protein environment. Lin and Truhlar [83] discuss questions such as: whether point charges in the MM region are appropriate for use in energy calculations; can the introduction of artificial link atoms in partitioning the QM and MM regions cause complications in energy calculations and geometry optimizations; do polarization effects between the atoms in the QM and MM regions of lead to issues in energy calculations; how does scaling of charges in the MM

region near the cut bonds, thus altering the net charge of the MM region, affect the energy calculation? Senn and Thiel [90] also discuss on how MM charges, placed near QM electron density, may cause overpolarization of the QM region.

Results in this study show distances and absorbances fluctuate with the size/contents of the QM region. It is not clear as to why changes in the QM region cause these differences in results. The changing number and/or types of amino acids included in the QM region could be impacting results. As well, when the QM region is expanded, so too is the boundary between the QM and MM regions, generating more cut and capped bonds, more scaling of charges in the MM region, and more area exposed to potential interactions between the QM and MM regions. These, and other factors, could be contributing to the variation in results.

Valuable information was obtained with QM/MM method, as applied in this study, through the *relative* comparison of computational results. Keeping computational parameters unchanged, it was observed that protonating Glu180 in one experiment, and turning off the charge of Glu180 in another, led to a significant red-shift of the absorption spectrum. While the absolute absorbance values obtained when Glu180 was protonated/unprotonated may not match experimental values, the magnitude of the wavelength shift observed is in agreement with experimental results and supports the assertion that Glu180 is the counterion in squid rhodopsin. Additionally, keeping

computational parameters unchanged, it was observed that changes made to two non-polar protein residues in Todarodes pacificus rhodopsin, Phe205 and Phe270, to represent polar residues in other species of squid, led to red-shifts of the absorption spectrum that are in agreement with those that are experimentally determined. Again, the calculated absolute absorbance values are relatively accurate for each of the species, the magnitude of the shifts in absorbance *between* the three species being quite consistent with those determined experimentally.

Suggestions for future studies would include further detailed investigation into the impact of experimental parameters on energy calculations in squid rhodopsin. The definition of the QM and MM regions (i.e. number and types of residues included, the linking atoms used, the scaling of charges), the choice of EE or ME scheme, the resultant interactions between the QM and MM regions and the effect of these interactions on energy calculations: all of these areas are ingredients of a complex problem whose components need to be understood in order to carry out absolute comparison of the change in energy between optimized rhodopsin models in a meaningful manner.

References

1. Schertler, G.F., *Signal transduction: the rhodopsin story continued.* Nature, 2008. **453**(7193): p. 292-3.
2. Murakami, M. and T. Kouyama, *Crystal structure of squid rhodopsin.* Nature, 2008. **453**(7193): p. 363-7.
3. Dreuw, A. and M. Head-Gordon, *Single-reference ab initio methods for the calculation of excited states of large molecules.* Chem Rev, 2005. **105**(11): p. 4009-37.
4. Frisch, M.J., et al., *Gaussian 09*, 2009, Gaussian, Inc.: Wallingford, CT, USA.
5. Hehre, W.J., *A Guide to Molecular Mechanics and Quantum Chemical Calculations*2003, Irvine: Wavefunction Inc. .
6. Atkins, P.W., *Physical Chemistry*. 5 ed1994, New York: W.H. Freeman and Company.
7. Warshel A., L., M., *Theoretical studies of enzymic reactions: Dielectric, electrostatic and steric stabilization of the carbonium ion in the reaction of lysozyme.* Journal of Molecular Biology 1976. **103**(2): p. 227-249.
8. Cramer, C.J., *Essentials of Computational Chemistry: Theories and Models*. 2nd ed2008, West Sussex: John Wiley & Sons, Ltd.
9. Masterton, W.L., Hurley, C. N. , *Chemistry: Principles and Reactions*. 2 ed1993, New York: Harcourt Brace Jovanovich Publishers.
10. Elliott, P.B., K., Furche, F. , *Excited states from time-dependent density functional theory.* Reviews in Computational Chemistry, 2007. **26**: p. 91-165.
11. Hofmann, K.P., et al., *A G protein-coupled receptor at work: the rhodopsin model.* Trends Biochem Sci, 2009. **34**(11): p. 540-52.
12. Stenkamp, R.E., D.C. Teller, and K. Palczewski, *Rhodopsin: a structural primer for G-protein coupled receptors.* Arch Pharm (Weinheim), 2005. **338**(5-6): p. 209-16.
13. Filipek, S., et al., *G protein-coupled receptor rhodopsin: a prospectus.* Annu Rev Physiol, 2003. **65**: p. 851-79.
14. Hubbard, R. and A. Kropf, *The Action of Light on Rhodopsin.* Proc Natl Acad Sci U S A, 1958. **44**(2): p. 130-9.
15. Shichida, Y. and T. Matsuyama, *Evolution of opsins and phototransduction.* Philos Trans R Soc Lond B Biol Sci, 2009. **364**(1531): p. 2881-95.
16. Suzuki, T., et al., *Immunochemical detection of GTP-binding protein in cephalopod photoreceptors by anti-peptide antibodies.* Zoolog Sci, 1993. **10**(3): p. 425-30.
17. Suzuki, T., et al., *Phosphatidyl inositol-phospholipase C in squid photoreceptor membrane is activated by stable metarhodopsin via GTP-binding protein, Gq.* Vision Res, 1995. **35**(8): p. 1011-7.
18. Pottinger, J.D., et al., *The identification and purification of the heterotrimeric GTP-binding protein from squid (Loligo forbesi) photoreceptors.* Biochem J, 1991. **279 (Pt 1)**: p. 323-6.
19. Rayer, B., M. Naynert, and H. Stieve, *Phototransduction: different mechanisms in vertebrates and invertebrates.* J Photochem Photobiol B, 1990. **7**(2-4): p. 107-48.

20. Baer, K.M. and H.R. Saibil, *Light- and GTP-activated hydrolysis of phosphatidylinositol bisphosphate in squid photoreceptor membranes.* J Biol Chem, 1988. **263**(1): p. 17-20.
21. Szuts, E.Z., et al., *Light stimulates the rapid formation of inositol trisphosphate in squid retinas.* Biochem J, 1986. **240**(3): p. 929-32.
22. Brown, J.E., et al., *myo-Inositol polyphosphate may be a messenger for visual excitation in Limulus photoreceptors.* Nature, 1984. **311**(5982): p. 160-3.
23. Fein, A., et al., *Photoreceptor excitation and adaptation by inositol 1,4,5-trisphosphate.* Nature, 1984. **311**(5982): p. 157-60.
24. Bhatia, J., et al., *Rhodopsin, Gq and phospholipase C activation in cephalopod photoreceptors.* J Photochem Photobiol B, 1996. **35**(1-2): p. 19-23.
25. Pepe, I.M., *Recent advances in our understanding of rhodopsin and phototransduction.* Prog Retin Eye Res, 2001. **20**(6): p. 733-59.
26. Fain, G.L., R. Hardie, and S.B. Laughlin, *Phototransduction and the evolution of photoreceptors.* Curr Biol, 2010. **20**(3): p. R114-24.
27. Wald, G., *Carotenoids and the Visual Cycle.* J Gen Physiol, 1935. **19**(2): p. 351-71.
28. Henderson, R. and P.N. Unwin, *Three-dimensional model of purple membrane obtained by electron microscopy.* Nature, 1975. **257**(5521): p. 28-32.
29. Ovchinnikov Iu, A., et al., *[Visual rhodopsin. III. Complete amino acid sequence and topography in a membrane].* Bioorg Khim, 1983. **9**(10): p. 1331-40.
30. Hargrave, P.A., et al., *The structure of bovine rhodopsin.* Biophys Struct Mech, 1983. **9**(4): p. 235-44.
31. Schertler, G.F., C. Villa, and R. Henderson, *Projection structure of rhodopsin.* Nature, 1993. **362**(6422): p. 770-2.
32. Hara-Nishimura, I., et al., *Cloning and nucleotide sequence of cDNA for rhodopsin of the squid Todarodes pacificus.* FEBS Lett, 1993. **317**(1-2): p. 5-11.
33. Wald, G., *The molecular basis of visual excitation.* Nature, 1968. **219**(5156): p. 800-7.
34. Collins, F.D., *Rhodopsin and indicator yellow.* Nature, 1953. **171**(4350): p. 469-71.
35. Morton, R.A. and G.A. Pitt, *Studies on rhodopsin. IX. pH and the hydrolysis of indicator yellow.* Biochem J, 1955. **59**(1): p. 128-34.
36. Matthews, R.G., et al., *Tautomeric Forms of Metarhodopsin.* J Gen Physiol, 1963. **47**: p. 215-40.
37. Wang, J.K., J.H. McDowell, and P.A. Hargrave, *Site of attachment of 11-cis-retinal in bovine rhodopsin.* Biochemistry, 1980. **19**(22): p. 5111-7.
38. Dratz, E.A., Hargrave, P. A. , *The structure of rhodopsin and the rod outer segment disk membrane.* Trends in Biochemical Sciences, 1983. **8**(4): p. 128-131.
39. Hargrave, P.A., et al., *Rhodopsin's protein and carbohydrate structure: selected aspects.* Vision Res, 1984. **24**(11): p. 1487-99.
40. Seidou, M., et al., *Amino acid sequence of the retinal binding site of squid visual pigment.* Biochim Biophys Acta, 1988. **957**(2): p. 318-21.
41. Sakmar, T.P., R.R. Franke, and H.G. Khorana, *Glutamic acid-113 serves as the retinylidene Schiff base counterion in bovine rhodopsin.* Proc Natl Acad Sci U S A, 1989. **86**(21): p. 8309-13.

42. Terakita, A., et al., *Counterion displacement in the molecular evolution of the rhodopsin family.* Nat Struct Mol Biol, 2004. **11**(3): p. 284-9.
43. Sekharan, S., A. Altun, and K. Morokuma, *Photochemistry of visual pigment in a G(q) protein-coupled receptor (GPCR)--insights from structural and spectral tuning studies on squid rhodopsin.* Chemistry, 2010. **16**(6): p. 1744-9.
44. Boll, F., *On the anatomy and physiology of the retina.* Vision Res, 1977. **17**(11-12): p. 1249-65.
45. Kuhne, W., *Chemical processes in the retina.* Vision Res, 1977. **17**(11-12): p. 1269-316.
46. Matthews, B.W., *Solvent content of protein crystals.* J Mol Biol, 1968. **33**(2): p. 491-7.
47. Levitt, M. and B.H. Park, *Water: now you see it, now you don't.* Structure, 1993. **1**(4): p. 223-6.
48. Schoenborn, B.P., A. Garcia, and R. Knott, *Hydration in protein crystallography.* Prog Biophys Mol Biol, 1995. **64**(2-3): p. 105-19.
49. Wald, G., J. Durell, and C.C. St George, *The light reaction in the bleaching of rhodopsin.* Science, 1950. **111**(2877): p. 179-81.
50. Grossfield, A., et al., *Internal hydration increases during activation of the G-protein-coupled receptor rhodopsin.* J Mol Biol, 2008. **381**(2): p. 478-86.
51. Angel, T.E., M.R. Chance, and K. Palczewski, *Conserved waters mediate structural and functional activation of family A (rhodopsin-like) G protein-coupled receptors.* Proc Natl Acad Sci U S A, 2009. **106**(21): p. 8555-60.
52. Jardon-Valadez, E., A.N. Bondar, and D.J. Tobias, *Dynamics of the internal water molecules in squid rhodopsin.* Biophys J, 2009. **96**(7): p. 2572-6.
53. Okada, T., et al., *Functional role of internal water molecules in rhodopsin revealed by X-ray crystallography.* Proc Natl Acad Sci U S A, 2002. **99**(9): p. 5982-7.
54. Okada, T., et al., *The retinal conformation and its environment in rhodopsin in light of a new 2.2 A crystal structure.* J Mol Biol, 2004. **342**(2): p. 571-83.
55. Ota, T., et al., *Structural changes in the Schiff base region of squid rhodopsin upon photoisomerization studied by low-temperature FTIR spectroscopy.* Biochemistry, 2006. **45**(9): p. 2845-51.
56. DeLange, F., et al., *Tyrosine structural changes detected during the photoactivation of rhodopsin.* J Biol Chem, 1998. **273**(37): p. 23735-9.
57. Nakagawa, M., et al., *How vertebrate and invertebrate visual pigments differ in their mechanism of photoactivation.* Proc Natl Acad Sci U S A, 1999. **96**(11): p. 6189-92.
58. Herzfeld, J., et al., *Solid-state 13C NMR study of tyrosine protonation in dark-adapted bacteriorhodopsin.* Biochemistry, 1990. **29**(23): p. 5567-74.
59. Roper, C.F.E., Sweeney M.J., Nauen C.E. , *FAO 1984 species catalogue. Cephalopods of the world. An annotated and illustrated catalogue of species of interest to fisheries.* FAO Fish. Synop. , 1984. **3**(125).
60. Warrant, E.J. and N.A. Locket, *Vision in the deep sea.* Biol Rev Camb Philos Soc, 2004. **79**(3): p. 671-712.
61. Munz, F.W., *Photosensitive pigments from the retinae of certain deep-sea fishes.* J Physiol, 1958. **140**(2): p. 220-35.

62. Denton, E.J. and F.J. Warren, *Visual pigments of deep-sea fish.* Nature, 1956. **178**(4541): p. 1059.
63. Hunt, D.M., et al., *The molecular basis for spectral tuning of rod visual pigments in deep-sea fish.* J Exp Biol, 2001. **204**(Pt 19): p. 3333-44.
64. Jerlov, N.G., *Marine Optics*. Elsevier Oceanography Series1976, New York: Elsevier.
65. Morris, A., J.K. Bowmaker, and D.M. Hunt, *The molecular basis of a spectral shift in the rhodopsins of two species of squid from different photic environments.* Proc Biol Sci, 1993. **254**(1341): p. 233-40.
66. Kawabata, A.e.a., *Spatial distribution of the Japanese common squid, Todarodes pacificus, during its northward migration in the western North Pacific Ocean.* Fisheries Oceanography, 2006. **15**(2): p. 113-124.
67. Suzuki, T., K. Uji, and Y. Kito, *Studies on cephalopod rhodopsin: photoisomerization of the chromophore.* Biochim Biophys Acta, 1976. **428**(2): p. 321-38.
68. Shichida, Y., F. Tokunaga, and T. Yoshizawa, *Circular dichroism of squid rhodopsin and its intermediates.* Biochim Biophys Acta, 1978. **504**(3): p. 413-30.
69. Hara, T. and R. Hara, *New photosensitive pigment found in the retina of the squid Ommastrephes.* Nature, 1965. **206**(991): p. 1331-4.
70. Hara T, H.R., *Electrical Conductance of Rhodopsin Solutions: Retinal degenerations, ERG, and optic pathways: proceedings of the 4th symposium of ISCER, September 1965.* Symp. Jpn. Opthalmol., 1966. **10**: p. 22-28.
71. Wlodawer, A., et al., *Protein crystallography for non-crystallographers, or how to get the best (but not more) from published macromolecular structures.* FEBS J, 2008. **275**(1): p. 1-21.
72. Costanzi, S., et al., *Rhodopsin and the others: a historical perspective on structural studies of G protein-coupled receptors.* Curr Pharm Des, 2009. **15**(35): p. 3994-4002.
73. Ponder, J.W., *TINKER*: Washington University, Saint Louis.
74. Ponder, J.W., Richards, F. M. , *An efficient newton-like method for molecular mechanics energy minimization of large molecules.* Journal of Computational Chemistry, 1987. **8**(7): p. 1016-1024.
75. Kollman, P., *AMBER*: University of California, San Francisco.
76. Wang, J., Cieplak, P. and Kollman, P. A., *How well does a restrained electrostatic potential (RESP) model perform in calculating conformational energies of organic and biological molecules?* J. Comput. Chem., 2000. **21**: p. 1049-1074.
77. Salomon-Ferrer, R.e.a., *An overview of the Amber biomolecular simulation package.* WIREs Comput Mol Sci 2012.
78. Elias, M., et al., *Hydrogen atoms in protein structures: high-resolution X-ray diffraction structure of the DFPase.* BMC Res Notes, 2013. **6**: p. 308.
79. *MAESTRO*, Schrodinger LLC: New York.
80. Hunt, P.; Available from: http://www.huntresearchgroup.org.uk/teaching/teaching_comp_lab_year3/3b_understand_opt.html.
81. Dapprich, S.e.a., *A new ONIOM implementation in Gaussian98. Part I. The*

calculation of energies, gradients, vibrational frequencies and electric field derivative. Journal of Molecular Structure (Theochem) 1999. **461-462**: p. 1-21.
82. Vreven, T., et al., *Geometry optimization with QM/MM, ONIOM, and other combined methods. I. Microiterations and constraints.* J Comput Chem, 2003. **24**(6): p. 760-9.
83. Lin, H., Truhlar, D. G. , *QM/MM: what have we learned, where are we, and where do we go from here?* Theoretical Chemistry Accounts 2007. **117**(2): p. 185-199.
84. Gascon, J.A. and V.S. Batista, *QM/MM study of energy storage and molecular rearrangements due to the primary event in vision.* Biophys J, 2004. **87**(5): p. 2931-41.
85. Yoshizawa, T. and Y. Shichida, *Low-temperature spectrophotometry of intermediates of rhodopsin.* Methods Enzymol, 1982. **81**: p. 333-54.
86. Kropf, A. and R. Hubbard, *The mechanism of bleaching rhodopsin.* Ann N Y Acad Sci, 1959. **74**(2): p. 266-80.
87. Solt, I., et al., *Evaluating boundary dependent errors in QM/MM simulations.* J Phys Chem B, 2009. **113**(17): p. 5728-35.
88. Han, M., B.S. DeDecker, and S.O. Smith, *Localization of the retinal protonated Schiff base counterion in rhodopsin.* Biophys J, 1993. **65**(2): p. 899-906.
89. Wanko, M., et al., *Calculating absorption shifts for retinal proteins: computational challenges.* J Phys Chem B, 2005. **109**(8): p. 3606-15.
90. Senn, H.M. and W. Thiel, *QM/MM methods for biomolecular systems.* Angew Chem Int Ed Engl, 2009. **48**(7): p. 1198-229.